Spectral densities of embedded interfaces in composite materials

A. R. McGurn
Department of Physics, Western Michigan University, Kalamazoo, Michigan 49008, USA

A. R. Day
Department of Biochemistry, Michigan State University, East Lansing, Michigan 48824-1116, USA

D. J. Bergman
School of Physics & Astronomy, Raymond and Beverly Sackler Faculty of Exact Sciences, Tel Aviv University, Tel Aviv 69978, Israel

L. C. Davis and M. F. Thorpe
Department of Physics and Astronomy, Michigan State University, East Lansing, Michigan 48824-1116, USA
(Received 5 March 2004; published 26 October 2004)

The effective resistivity and conductivity of two media that meet at a randomly rough interface are computed in the quasistatic limit. The results are presented in the spectral density representations of the Bergman-Milton formulation for the properties of two-component composite materials. The spectral densities are extracted from computer simulations of resistor networks in which the random interface separates two regions containing different types of resistors. In the limit that the bond lengths in the resistor network are small compared to parameters characterizing the surface roughness, the resistor network simulation approximates the continuum limit of the two-component composite. The Bergman-Milton formulation is used to obtain a set of exact sum rules in the continuum limit for the spectral densities in terms of parameters describing the surface roughness and the simulation results are found to agree with these limiting forms. Perturbation theory results of the composite in the continuum limit for weakly rough random interfaces are also presented. An expansion of the spectral density is determined to second order in the surface profile function of the random interface and compared with the Bergman-Milton sum rules and computer simulation results. The formalism is applied to surface plasmons, electron energy loss, and light scattering from rough surfaces. Layered structures are discussed briefly.

DOI: 10.1103/PhysRevB.70.144205 PACS number(s): 41.20.Cv, 71.36.+c, 77.55.+f, 02.70.Hm

I. INTRODUCTION

The theory of the conductivity and resistivity of composite materials has a long history. Earliest considerations (see, e.g., the book by Sihvola[1]) were based on simple analytical methods. These emphasized exactly solvable models, perturbation treatments, and effective medium approximations. Modern theories have focused on more sophisticated analytical treatments[2–12] and on computer simulations.[6–10,13–19] Of particular interest to us in this paper is the formulation of Bergman and Milton, first published in Refs. 3 and 4, and later in greater detail in a lecture notes volume,[5] for calculating the conductivity and resistivity properties of two-component composite materials. This method is based on a formal solution of Gauss's Law and has yielded a number of exact inequalities, limiting forms, and sum rules for two-component composites. In this "spectral treatment," the formal solution for the average conductivity and resistivity of the composite system are expressed as functions of the conductivities or resistivities of its two-components in terms of an integral (Hilbert) transform involving a spectral density and a simple pole, or an entire sequence of simple poles in the case of a periodic microstructure. The physics of the solution is in the spectral density which depends on the geometry of the constituent materials of the composite. Once the spectral density is known the effective conductivity and resistivity properties of the system are determined for all possible values of the resistivities and conductivities of the two components forming the system. The spectral density is difficult in general to compute and has only been determined exactly for restricted geometries. Some analytical and numerical results are also available in perturbation theory and moment expansions and for special cases.[3,4,6–10,13,14,17–23] Although the spectral density in general cannot be calculated by analytical means, developments in computer simulation techniques[7,24–30] now allow for the numerical determination of the spectral density.[14,18,19,24–28,31] Spectral density methods are found to be of great generality and have been applied to a wide variety of different systems. These include randomly disordered materials,[8–10,13,14,18–20,24–28,31] periodically ordered materials,[6–10,21–23] and those with isolated impurities of a regular geometry.[1,8–10,24,25]

Resistor network simulations can greatly facilitate the study of spectral densities of two-component composites.[18,19,32] One of the earliest many-body problems treated by means of computer simulations is the resistor network problem.[13] This involves the numerical determination of the resistivity of a mixed network of resistors, and is of interest as a model for random alloys, particularly when the length of a resistor in the network is small compared to typical length scales in the alloy. The resistor network problem has interesting transport and phase transition properties, which have led to the development of a number of efficient algorithms for the quick solution of large arrays of mixed

resistors. These algorithms are now finding application with the Bergman-Milton formulation.[18–28,31,32] The first use of resistors arrays to extract the spectral density of two-component alloys was in the paper of Day and Thorpe.[18] In this paper a general two-dimensional alloy was treated and the features of the spectral density determined for a wide variety of disorders.[18,19,32] This spectral density approach was also used to model the optical properties of a two-component material.[32]

Here the Day and Thorpe method is used to determine the continuum limit of the spectral density in the Bergman-Milton formulation for the resistivity and conductivity of two media that meet at a randomly rough buried interface. For simplicity, the interface between the two different resistive or conducting media is described by a one-dimensional Gaussian random profile function so that the interface retains translational symmetry along one axis in space.[33,34] Generalizations to two-dimensionally rough surfaces can be made, but require much more computational effort.[34] The treatment of more general surface roughness statistics is straightforward and the choice of Gaussian random statistics is discussed later in the text. The calculations are for the low frequency limit of the conductivity or resistivity in which the displacement current is ignored, and are done by using a combination of resistor network simulations and analytical techniques. Comparison of the spectral density results from simulation data is made with a variety of analytical limiting forms.

The bulk of the results in this paper for the random interface in a two-component composite are obtained from resistor network simulations involving systems with bond disorder. The coordinates of a Gaussian randomly disordered interface are generated and are then used to separate two regions of different resistor types. In the limit that the parameters characterizing the rough interface between the two regions of different resistor bonds are large compared to the bond lengths, the continuum limit is well approximated. The spectral density in the continuum limit is extracted from computer simulation results. The Bergman-Milton theory is used to generate a number of sum rules obeyed by the continuum limit of the spectral density for the interface. (It is important to note, in regard to the Bergman-Milton theory, that the exact sum rules usually apply away from the continuum limit as well. We believe that this is true for the resistor networks studied here.) These results, which are of interest in themselves, are used to check the simulation data.

Perturbation theory results for the continuum limit of the interface problem are generated in the limit of weak roughness. The expansion parameter is the surface profile function, which is represented by a set of Gaussian random stationary functions. An expression for the spectral density to second order in the surface profile function is obtained and found to agree with the Bergman-Milton sum rules and the results of the computer simulation.

The order of the paper is: In Sec. II, the continuum model is presented and discussed, using a spectral formulation of the Bergman-Milton type, and a number of sum rules are derived. In Sec. III, the computer simulation is discussed. Results for the spectral densities are presented, and a comparison is made with the limiting forms obtained in Sec. II. Perturbation theory for weakly rough interfaces is presented in Sec. IV. In Sec. V, applications are made to surface plasmons, electron energy, and light scattering from rough surfaces. Generalizations of the theory to treat multiple layered media are in Sec. VI. A general discussion of the results is given in Sec. VII.

II. SPECTRAL FORMULATION

Consider a quasistatic system between two parallel plates. The upper $z=L/2$ plate is at a potential V_0, and the lower $z=-L/2$ plate is at zero potential. Between the parallel plates are two media of conductivities σ_1 and σ_2 (resistivities ρ_1 and ρ_2) separated by a (two-dimensional) interface that is rough in one of its two dimensions. Two geometries are treated: In the first, the average of the rough surface separating the two media is the y-z plane. For this geometry the effective conductivity of the medium between the parallel plates is calculated. In the second, the average of the rough surface separating the two media is the x-y plane. For this geometry the effective resistivity of the medium between the parallel plates is calculated.

In both geometries the average electric field is defined by[2,6]

$$\vec{E}_0 = \frac{1}{V}\int \vec{E}(\vec{r})d^3r, \tag{1}$$

where $\vec{E}(\vec{r})$ is the field between the parallel plates, $\vec{E}_0 = \mathbf{e}_z V_0/L$, and V is the volume between the plates. The effective conductivity σ^{eff} of the medium between the parallel plates is then defined by

$$\vec{J}_0 = \sigma^{eff}\vec{E}_0 = \frac{1}{V}\int \vec{J}d^3r, \tag{2}$$

with the effective resistivity related to σ^{eff} by $\rho^{eff}=1/\sigma^{eff}$.

A. Average interface in the *y-z* plane

In this geometry the position-dependent conductivity of the medium between the parallel plates is given by

$$\sigma(\vec{r}) = \sigma_2\left[1 - \frac{1}{s}\theta_1(\vec{r})\right], \tag{3}$$

where $s=\sigma_2/(\sigma_2-\sigma_1)$. Here

$$\theta_1(\vec{r}) = \begin{cases} 1, & x < \xi(z) \\ 0, & \text{otherwise}, \end{cases} \tag{4}$$

where $x=\xi(z)$ defines the one-dimensionally rough interface profile. (Note: the surface is translationally invariant in the y direction.) For a flat interface, $\theta_1(\vec{r})$ in Eq. (3) is replaced by $\theta_{10}(\vec{r})$ defined by

$$\theta_{10}(\vec{r}) = \begin{cases} 1, & x < 0 \\ 0, & \text{otherwise}. \end{cases} \tag{5}$$

In the following, systems with both random and flat interfaces are considered. In both systems, the volume fraction of material with conductivity σ_1 is p_1 and the volume fraction of material with conductivity σ_2 is p_2.

The one-dimensionally randomly rough interface in Eq. (4) is defined by $x=\xi(z)$, where $\xi(z)$ is from a set of Gaussian random functions $\{\xi(z)\}$. This set is chosen to have specific statistical properties that are ultimately correlated with the average physical properties of the random system. The average physical properties of the random system are determined by averaging these properties computed as functionals of $\xi(z)$ over the set of functions $\{\xi(z)\}$.

The set of Gaussian random functions $\{\xi(z)\}$ satisfy[33,34]

$$\langle \xi(z) \rangle = 0, \tag{6}$$

$$\langle \xi(z)\xi(z') \rangle = \delta^2 \exp(-|z-z'|^2/a^2), \tag{7}$$

where $\langle\ \rangle$ indicates an average over $\{\xi(z)\}$, δ is the rms deviation from a flat surface, and a is the correlation length of the surface roughness. Higher order correlation functions of the Gaussian surface roughness are expressed in the usual way,[33,34] in terms of those in Eqs. (6) and (7) as the sum of all possible pair and singlet contracted averages. For example, $\langle \xi(z)\xi(z')\xi(z'') \rangle = 0$ and

$$\begin{aligned}\langle \xi(z)\xi(z')\xi(z'')\xi(z''') \rangle = {} & \langle \xi(z)\xi(z') \rangle \langle \xi(z'')\xi(z''') \rangle + \langle \xi(z)\xi(z'') \rangle \\ & \times \langle \xi(z')\xi(z''') \rangle + \langle \xi(z)\xi(z''') \rangle \\ & \times \langle \xi(z')\xi(z'') \rangle .\end{aligned}$$

A reason that Gaussian random functions have become popular in the study of disordered systems is that they give rise to perturbation treatments which have a Wick's Theorem. This allows for a simple diagrammatic treatment.

To determine the effective conductivity from Eqs. (1) and (2), the electric field of the disordered medium is written as $\vec{E}=-E_0\nabla\phi$, where $E_0=|\vec{E}_0|$ and $E_0\phi$ is the electric potential. From the current continuity, the function ϕ is a solution of

$$\nabla \cdot [\sigma(\vec{r})\nabla\phi] = 0, \tag{8}$$

subject to the boundary conditions $\phi(z=L/2)=\phi_0=L$, $\phi(z=-L/2)=0$. Using Eqs. (3)–(5) in Eq. (8) gives

$$\nabla \cdot \left[\left(1 - \frac{1}{s}\theta_{10} \right) \nabla\phi \right] = \frac{1}{s} \nabla \cdot (\theta_3 \nabla\phi), \tag{9}$$

where $\theta_3(\vec{r})=\theta_1(\vec{r})-\theta_{10}(\vec{r})$. A formal solution of Eq. (9) for ϕ is

$$\begin{aligned}\phi(\vec{r}) &= z + \frac{L}{2} - \int d^3r' G(\vec{r},\vec{r'}|s) \frac{1}{s} \nabla' \cdot [\theta_3(\vec{r'}) \nabla' \phi(\vec{r'})] \\ &= z + \frac{L}{2} + \frac{1}{s} \int d^3r'\, \theta_3(\vec{r'}) \nabla' G(\vec{r},\vec{r'}|s) \cdot \nabla' \phi(\vec{r'}).\end{aligned} \tag{10}$$

Here the Green's function $G(\vec{r},\vec{r'}|s)$ satisfies

$$\nabla \cdot \left[1 - \frac{1}{s}\theta_{10}(\vec{r}) \right] \nabla G(\vec{r},\vec{r'}|s) = -\delta^{(3)}(\vec{r}-\vec{r'}) \tag{11}$$

in V, subject to the boundary condition that $G=0$ on the surface of V. Equation (10) can be written in a compact operator notation as

$$\phi = z + \frac{L}{2} + \frac{1}{s}\hat{\Gamma}(s)\phi, \tag{12}$$

where $\hat{\Gamma}(s)\phi = \int d^3r'\, \theta_3(\vec{r'}) \nabla' G(\vec{r},\vec{r'}|s) \cdot \nabla' \phi(\vec{r'})$.

Using an alternative formulation developed for general random two-component composites,[2,6–10,14,18,19,35–37] ϕ can also be written as

$$\phi = z + \frac{L}{2} + \sum_i \frac{f_i s_i}{s - s_i} \phi_i. \tag{13}$$

Here $f_i = (1/V) \int d^3r\, \theta_1(\vec{r}) \nabla\phi_i(\vec{r}) \cdot \nabla[z+(L/2)]$ and ϕ_i are the solutions of the Hermitian eigenvalue problem

$$\hat{\Gamma}_0 \phi_i = s_i \phi_i, \tag{14}$$

where

$$\hat{\Gamma}_0 \phi_i = \int d^3r'\, \theta_1(\vec{r'}) \nabla' G_0(\vec{r},\vec{r'}) \cdot \nabla' \phi_i(\vec{r'}), \tag{15}$$

for $\nabla^2 G_0(\vec{r},\vec{r'}) = -\delta^{(3)}(\vec{r}-\vec{r'})$. Equation (13) is found to be useful below as it explicitly exhibits the pole structure of the dependence of ϕ on s.

The effective conductivity of the system is computed by using the formal solution of ϕ [either Eq. (12) or (13)] in Eqs. (1) and (2). The average electric field is along the z direction, so that

$$\sigma^{eff} = \frac{1}{VE_0} \int d^3r (-\hat{k} \cdot \sigma\vec{E}), \tag{16}$$

and from Eqs. (3) and (16)

$$\sigma^{eff} = \frac{\sigma_2}{VE_0} \left[\int d^3r \left(1 - \frac{1}{s}\theta_{10} \right) (-\hat{k} \cdot \vec{E}) - \frac{1}{s} \int d^3r\, \theta_3 (-\hat{k} \cdot \vec{E}) \right]. \tag{17}$$

The electric field in the first integral in Eq. (17) can be replaced by $\vec{E}_0$ so that from Eqs. (12) and (17),

$$\frac{\sigma^{eff}}{\sigma_2} = p_1 \frac{\sigma_1}{\sigma_2} + p_2 - \frac{1}{s^2} \left\langle z + \frac{L}{2} \middle| \hat{\Gamma}(s)\phi \right\rangle, \tag{18}$$

where $\langle f|g\rangle = (1/V) \int d^3r\, \theta_3(\vec{r}) \nabla f \cdot \nabla g$. We note that, in spite of the similar notation, the expression $\langle f|g\rangle$ is not a scalar product, since $\theta_3(\vec{r})$ takes on the negative value −1 as well as the positive values +1: It has to, because its volume average vanishes. This separates σ^{eff} into two contributions: the results for a flat surface and a component arising from the disorder. Alternatively, from Eqs. (13) and (16), we find that

$$\frac{\sigma^{eff}}{\sigma_2} = 1 - \sum_i \frac{F_i}{s - s_i}, \tag{19}$$

where $F_i = |f_i|^2$. This expresses σ^{eff} in terms of the eigenvalues $\{\phi_i\}$ and eigenvectors $\{s_i\}$ of Eq. (14).

Following the formulation used to study the effective conductivity of a general three-dimensional, two-component composite,[2,6,7] we define the function $F(s)$ by

$$F(s) = 1 - \frac{\sigma^{eff}}{\sigma_2}. \tag{20}$$

Here σ^{eff} is the effective conductivity of the medium in the presence of a randomly rough interface. For the flat surface Eq. (20) becomes

$$F_0(s) = 1 - \frac{\sigma_0^{eff}}{\sigma_2} = \frac{p_1}{s}, \tag{21}$$

where $\sigma_0^{eff} = p_1\sigma_1 + p_2\sigma_2$ is the effective conductivity in this limit. To study the effects of the rough interface, it is most useful to determine the difference of these two functions, i.e.,

$$F(s) - F_0(s) = \frac{\sigma_0^{eff} - \sigma^{eff}}{\sigma_2}. \tag{22}$$

In the formulation of Eqs. (12), (16), and (18), this becomes

$$F(s) - F_0(s) = \frac{1}{s^2}\left\langle z + \frac{L}{2}\middle|\hat{\Gamma}(s)\phi\right\rangle = \frac{1}{s}\left\langle z + \frac{L}{2}\middle|\frac{\hat{\Gamma}(s)}{s - \hat{\Gamma}(s)}\middle| z + \frac{L}{2}\right\rangle. \tag{23}$$

In the formulation of Eqs. (13), (16), and (19), Eq. (22) becomes

$$F(s) - F_0(s) = \frac{1}{s}\sum_i \frac{F_i s_i}{s - s_i} = \int_0^1 du \frac{g_\sigma(u)}{s(s-u)}, \tag{24}$$

where $g_\sigma(u)$ is the spectral density. The second equality of Eq. (24) is a generalization of the first equality: It includes the first equality as a special case, but is also applicable when the pole spectrum ceases to be discrete. That enables us to apply this formalism also to spectral functions $F(s)$, which are obtained by averaging over an ensemble of similar systems. Equation (24) shows that the function $F(s) - F_0(s)$ is determined by a set of simple poles in s. These poles appear at the eigenvalues of Eq. (14), and are weighted by the spectral density $F_i s_i$ or $g_\sigma(u)$. The spectral density then determines the properties of the system as a function of s and contains the essential physics of the system. The goal of our computer simulation studies will be the determination of this spectral density for random rough interfaces and the determination of how the general features of the spectral density are influenced by the nature of the disorder of the randomly rough interface.

B. Average interface in the *x-y* plane

In this geometry, the resistivity of the medium between the parallel plates in the presence of a randomly rough interface is given by

$$\rho(\vec{r}) = \rho_2\left[1 - \frac{1}{t}\theta_1(\vec{r})\right] \tag{25}$$

for $t = \rho_2/(\rho_2 - \rho_1)$ and

$$\theta_1(\vec{r}) = \begin{cases} 1, & z < \xi(x) \\ 0, & \text{otherwise} \end{cases}. \tag{26}$$

Here $\{\xi(x)\}$ are a set of Gaussian random functions defining the interface profile. For a flat interface, $\theta_1(\vec{r})$ in Eq. (25) is replaced by $\theta_{10}(\vec{r})$, which is defined as in Eq. (26), but with the $z < \xi(x)$ condition replaced by $z < 0$. For these two systems, the volume fraction of ρ_1 is p_1 and the volume fraction of ρ_2 is p_2.

From the current continuity equation $\nabla \cdot \vec{J} = 0$, it follows that the current density can be written in terms of a vector potential, i.e., $\vec{J} = \nabla \times \vec{A}$.[6] The quasistatic limit of Faraday's law $\nabla \times \vec{E} = 0$ then gives

$$\nabla \times [\rho(\vec{r})\nabla \times \vec{A}] = 0, \tag{27}$$

which defines $\vec{A}$ in V. This equation is solved for $\vec{A}$ subject to the boundary condition that on the surface of V, $\hat{n} \times \vec{A} = \frac{1}{2}[\hat{n} \times (\vec{J}_{0z} \times \vec{r})]$ where $\hat{n}$ is a unit normal out of V.

Equation (27) can be rewritten as

$$\nabla \times \left\{\left(1 - \frac{1}{t}\theta_{10}\right)\nabla \times \vec{A}\right\} = \frac{1}{t}\nabla \times \{\theta_3(\vec{r})\nabla \times \vec{A}\}, \tag{28}$$

where $\theta_3(\vec{r}) = \theta_1(\vec{r}) - \theta_{10}(\vec{r})$. Defining a Green's function tensor, $\vec{\vec{G}}(\vec{r}, \vec{r}'|s, k)$, in V by

$$-\nabla \times \left\{\left[1 - \frac{1}{t}\theta_{10}(\vec{r})\right]\nabla \times \vec{\vec{G}}(\vec{r}, \vec{r}'|t, k)\right\} + k^2\vec{\vec{G}}(\vec{r}, \vec{r}'|t, k) = -\delta^{(3)}(\vec{r} - \vec{r}')\mathbb{1}, \tag{29}$$

subject to $\hat{n} \times \vec{\vec{G}} = 0$ on the surface of V, we can form the function

$$\vec{A}(\vec{r}, k) = \vec{A}^0(\vec{r}) + \frac{1}{t}\int d^3r' \vec{\vec{G}}(\vec{r}, \vec{r}') \cdot \nabla' \times \{\theta_3(\vec{r}')(\nabla' \times \vec{A}'(\vec{r}', k)\} = \vec{A}^0(\vec{r}) + \frac{1}{t}\int d^3r' \theta_3(\vec{r}')[\nabla' \times \vec{\vec{G}}(\vec{r}, \vec{r}')] \cdot [\nabla' \times \vec{A}'(\vec{r}', k)], \tag{30}$$

where $\vec{A}^0(\vec{r}) = (\vec{J}_{0z} \times \vec{r})/2$ is the solution for a smooth interface. Taking the $k \to 0$ limit of the right-hand side of the second equality in Eq. (30) gives a formal solution of Eq. (28) for $\vec{A}(\vec{r})$. Care must be taken in treating the $k \to 0$ limit in Eq. (30) as in this limit $\vec{\vec{G}}(\vec{r}, \vec{r}'|t, k)$ does not exist even

though $\nabla' \times \overleftrightarrow{G}(\vec{r},\vec{r}'|t,k)$ does exist. This is not a problem as we will only need $\nabla' \times \overleftrightarrow{G}(\vec{r},\vec{r}'|t,k)$ in the results below. Equation (30) can be rewritten in operator notation as

$$\vec{A} = \vec{A}^0 + \frac{1}{t}\overleftrightarrow{\Gamma}\vec{A}, \tag{31}$$

so that

$$\vec{A} = \vec{A}^0 + \frac{\mathbb{1}}{t\mathbb{1} - \overleftrightarrow{\Gamma}}\overleftrightarrow{\Gamma}\vec{A}^0. \tag{32}$$

Using the standard form of the general two-composite theory,[6] an alternative expression for $\vec{A}$ can be given in terms of the solutions of a Hermitian eigenvalue problem. From the Hermitian eigenvalue problem

$$\overleftrightarrow{\Gamma}_0\vec{A}_i = t_i\vec{A}_i, \tag{33}$$

where

$$\overleftrightarrow{\Gamma}_0\vec{A}_i = \int d^3r'\,\theta_1(\vec{r}')[\nabla' \times \overleftrightarrow{G}_0(\vec{r},\vec{r}')] \cdot [\nabla' \times \vec{A}_i(\vec{r}')] \tag{34}$$

for $\overleftrightarrow{G}_0(\vec{r},\vec{r}') = \lim_{k\to 0}\overleftrightarrow{G}_1(\vec{r},\vec{r}')$ with $(-\nabla\times\nabla + k^2)\overleftrightarrow{G}_1(\vec{r},\vec{r}') = -\delta^{(3)}(\vec{r}-\vec{r}')$, it follows that

$$\vec{A} = \vec{A}^0 + \sum_i \frac{h_i t_i}{t - t_i}\vec{A}_i, \tag{35}$$

where $h_i = (1/V)\int d^3r\,\theta_1(\vec{r})(\nabla\times\vec{A}_i)\cdot(\nabla\times\vec{A}^0)$. From Eq. (35) it is seen that $\vec{A}$ as a function of t is composed of simple poles.

The effective resistivity is given by

$$\rho^{eff} = \frac{1}{VJ_0^2}\int d^3r\rho\vec{J}_0\cdot\vec{J}. \tag{36}$$

The integral in Eq. (36) can be rewritten as

$$\int d^3r\rho\vec{J}_0\cdot\vec{J} = \rho_2\int d^3r\left(1 - \frac{1}{t}\theta_{10}\right)\vec{J}_0\cdot\vec{J} - \frac{\rho_2}{t}\int d^3r\,\theta_3\vec{J}_0\cdot\vec{J}$$
$$= V\rho_0^{eff}J_0^2 - \frac{\rho_2}{t}\int d^3r\,\theta_3\vec{J}_0\cdot\vec{J}, \tag{37}$$

where ρ_0^{eff} is the effective resistivity of the flat surface. Writing $\vec{J} = \vec{J}_0 + (\vec{J} - \vec{J}_0)$ and using the fact that θ_3 averages to zero over the surface, from Eqs. (31), (32), (36), and (37) we find that

$$\frac{\rho^{eff}}{\rho_2} = \frac{\rho_0^{eff}}{\rho_2} - \frac{1}{tV}\frac{1}{J_0^2}\int d^3r\,\theta_3\vec{J}_0\cdot(\vec{J} - \vec{J}_0)$$
$$= \frac{\rho_0^{eff}}{\rho_2} - \frac{1}{tV}\frac{1}{J_0^2}\int d^3r\,\theta_3(\nabla\times\vec{A}^0)\cdot(\nabla\times\vec{B}). \tag{38}$$

Here, from Eqs. (31) and (32), $\vec{B} = [\mathbb{1}/(t\mathbb{1} - \overleftrightarrow{\Gamma})]\overleftrightarrow{\Gamma}\vec{A}^0$. Alternatively, from the form for $\vec{A}$ given in Eq. (35), it can be shown that

$$\frac{\rho^{eff}}{\rho_2} = 1 - \sum_i \frac{H_i}{t - t_i}, \tag{39}$$

where $H_i = (1/J_0^2)|h_i|^2$.

By analogy with resistivity studies of composite materials, we define a function $H(t)$ for the rough interface by[6]

$$H(t) = 1 - \frac{\rho^{eff}}{\rho_2}, \tag{40}$$

and for the flat interface a function $H_0(t)$ by

$$H_0(t) = 1 - \frac{\rho_0^{eff}}{\rho_2}. \tag{41}$$

For the interface problem it is useful to study the difference of these two functions, i.e., $H(t) - H_0(t)$. From the formulation in Eqs. (31) and (32) it is found that

$$H(t) - H_0(t) = \frac{1}{t}\langle\vec{A}^0|\frac{\overleftrightarrow{\Gamma}(t)}{t\mathbb{1} - \overleftrightarrow{\Gamma}(t)}|\vec{A}^0\rangle, \tag{42}$$

where $\langle\vec{f}|\vec{g}\rangle = (1/VJ_0)\int d^3r\,\theta_3(\vec{r})(\nabla\times\vec{f})\cdot(\nabla\times\vec{g})$. This form of $H(t) - H_0(t)$ is used below to obtain an asymptotic limit. From Eqs. (33)–(35) we find

$$H(t) - H_0(t) = \frac{1}{t}\sum_i \frac{H_i t_i}{t - t_i} = \int dv\,\frac{g_\rho(v)}{t(t - v)}. \tag{43}$$

The second equality of Eq. (43) introduces the spectral density $g_\rho(v)$. This equality is a generalization of the first equality of that equation, in the same way and for the same reasons that were explained for the second equality of Eq. (24). As with the conductivity problem, the essential physics of the effective resistivity of the composite is contained in $g_\rho(v)$. The function $H(t) - H_0(t)$ has a structure that is very similar to that of $F(s) - F_0(s)$. As a function of t, it is determined as a sum of simple poles which occur at the eigenvalues $\{t_i\}$ of the operator $\hat{\Gamma}(t)$. The spectral density $H_i t_i$ or $g_\rho(v)$ will be determined numerically below for a variety of randomly rough interfaces.

C. Sum rules

To obtain a first sum rule for the effective conductivity in subsection A, consider $F(s) - F_0(s)$ in Eqs. (23) and (24). Multiplying Eq. (24) by s^2 and taking the limit that $s\to\infty$ gives

$$C(\delta,a) = \lim_{s\to\infty} s^2[F(s) - F_0(s)] \to \sum_i F_i s_i. \tag{44}$$

Multiplying Eq. (23) by s^2, we find that in this limit

$$s^2[F(s)-F_0(s)] \to \left\langle z+\frac{L}{2}\middle|\,\hat{\Gamma}(\infty)\,\middle|z+\frac{L}{2}\right\rangle = \frac{1}{V}\int d^3r \int d^3r'\,\theta_3(\vec{r})\theta_3(\vec{r'})\frac{\partial}{\partial z}\frac{\partial}{\partial z'}G_0(\vec{r},\vec{r'}) \propto \frac{1}{V}\int d^3r|\theta_3(\vec{r})| = O(p_3), \tag{45}$$

where p_3 is the (small) volume fraction occupied by the rough interface: It would have an accurately defined value if the roughness were defined by a sharp interface, but its value can also be defined, in the case of a Gaussian-distributed set of interface functions $\xi(\vec{r})$ [see Eqs. (6) and (7)]. For a Gaussian-distributed sharp interface two limiting behaviors of p_3 are observed. For $\delta/a \ll 1$, p_3 is expected to be proportional to $\delta^2/(La)$. This arises from the fact that p_3 should go to zero as δ goes to zero and as L or a become infinite. (Note: When $a \to \infty$, the Gaussian random surface tends to a flat surface.) For $\delta/a \gg 1$, p_3 is expected to be proportional to δ/L: In this limit, a feature of length $2a$ on the surface contributes an area to $\int dxdy|\theta_3(\vec{r})|$, which is of order $2a|\delta|$. There are $L/2a$ such lengths along the interface, so that the total area along the random interface is δL and p_3 goes as δ/L. A possible form that would interpolate between these two limits would be, e.g., $p_3 \propto \delta^2/[(La)(1+c\delta/a)]$ for some positive constant c. In Eq. (45) $G_0(\vec{r},\vec{r'})$ is the $s \to \infty$ limit of the Green function defined in Eq. (11).

A second sum rule on $F(s)$ is the well known rule[2,6] $\Sigma_i F_i = p_1$. This is used in Eq. (24) to relate the residue of the pole at $s=0$ to those for $s_i \neq 0$. Denoting the residue at zero in Eq. (24) by w_σ, we find that

$$w_\sigma = -\sum_i{}' F_i = F_0 - p_1, \tag{46}$$

where the prime in Eq. (46) indicates that the $i=0$ term [i.e., the residue F_0 of the pole $s_0=0$ of Eq. (19)] is not included in the sum.

Similar results for $H(t)-H_0(t)$ can be obtained from Eqs. (42) and (43). Multiplying Eq. (43) by t^2 gives in the $t \to \infty$ limit

$$R(\delta,a) = \lim_{t\to\infty} t^2[H(t)-H_0(t)] \to \sum_i H_i t_i, \tag{47}$$

and doing the same to Eq. (42) gives

$$t^2[H(t)-H_0(t)] \to -\frac{1}{V}\int d^3r \int d^3r'\,\theta_3(\vec{r})\theta_3(\vec{r'})\left(\frac{\partial^2}{\partial x^2}+\frac{\partial^2}{\partial y^2}\right) \times G_0(\vec{r},\vec{r'}) \propto \frac{1}{V}\int d^3r|\theta_3(\vec{r})|. \tag{48}$$

A second sum rule on $H(t)$ is given from Eqs. (43),[6] and relates the residue at $t=0$ (denoted by w_ρ) to the sum of the residues of the nonzero poles by

$$w_\rho = -\sum_i{}' H_i = H_0 - p_1, \tag{49}$$

where the prime notation in Eq. (46) is again used for the sum in Eq. (49) and H_0 denotes the residue of the pole at $t_0=0$ in Eq. (39).

III. COMPUTER RESULTS

Following the treatment of Day and Thorpe,[18,19,31,32] the spectral densities defined in Eqs. (22)–(24) and (40)–(43) are extracted from computer simulation studies of two-dimensional resistor networks. In this extraction, a square lattice network of resistor bonds between two perfectly conducting plates is considered. The vertices at which the resistors meet are labeled by (x,z) space coordinates and the conducting plates are parallel to the x-y plane. The random interface separating regions of two different resistor types is given by specifying $[\xi(z),z]$ for the consideration of the system defined in Sec. II A, or specifying $[x,\xi(x)]$ for consideration of the system defined in Sec. II B.

The details of the algorithm used to extract the spectral density from resistor network data are discussed elsewhere.[14,18,19,31,32] Consequently, only a brief outline of the workings of the code will be given here. This will be followed by a detailed description of the resistor networks, a discussion of the generation of the random interface, and the presentation of the numerical results for the spectral density of the buried interfaces.

The spectral densities are extracted from Eqs. (24) and (43) using the analytical properties of $F(s)$ and $H(t)$ in the complex s or t plane. $F(s)$ and $H(t)$ are real for s and t real and, except for a set of simple poles that occur on the real axis in the interval $0 \leqslant s \leqslant 1$ or $0 \leqslant t \leqslant 1$, are analytic in the general complex plane. By numerically computing $F(s)$ and $H(t)$ for values of s and t slightly off the real axis, the relationship

$$\lim_{\epsilon\to 0}\int dx\frac{f(x)}{x-b+i\epsilon} = P\int dx\frac{f(x)}{x-b} - i\pi f(b) \tag{50}$$

can be used to extract the spectral density from the imaginary parts of the numerical data. $F(s)$ and $H(t)$ are related to the effective resistivity and conductivity, so that one of the many algorithms available to compute the effective resistivity and conductivity of a network of complex valued resistors can be used for their determination. In particular, the algorithm of Ref. 14 was used for the results presented below.

We have considered a square lattice resistor array of 128×128 resistor bonds. The functions $F(s)$ and $H(t)$ were computed for a net of s and t values given by $s_n = n\Delta s + i\epsilon$ and $t_n = n\Delta t + i\epsilon$, where $\Delta s = 0.005$, $\Delta t = 0.005$, and $\epsilon = 0.003$. To generate spectral densities 500 realizations of the Gaussian random interface with statistical properties characterized by the parameters δ and a defined in Eqs. (6) and (7) were used. The coordinates of the Gaussian random interface—$[\xi(z),z]$ for the $F(s)$ calculation and $[x,\xi(x)]$ for the $H(t)$ calculations—were computed using the algorithm described in Ref. 34. In order to approximate the continuum limit of

the two-component composite system by the resistor network, a series of runs were generated for constant δ/a. As δ and a were increased for fixed δ/a, the spectral density divided by $C(\delta,a)=\lim_{s\to\infty} s^2[F(s)-F_0(s)]$ or $R(\delta,a)=\lim_{t\to\infty} t^2[H(t)-H_0(t)]$ was found to approach a limiting form. For fixed δ/a, the volume fraction of material between the random rough surface and the *y-z* (or *x-y*) plane scales with $\delta^2/(La)$, so that the continuum limit of the spectral density divided by $C(\delta,a)$ and $R(\delta,a)$ should be a constant. The limiting form of the spectral density normalized by Eq. (44) or Eq. (47) generated from the resistor network results should agree with the continuum limit result when the lengths characterizing the interface roughness are large compared to those of the resistor bonds.

As a check on the numerically generated data, the sum rules of Sec. II C were evaluated. The poles at $s=0$ ($t=0$) in $F(s)[H(t)]$ were obtained from the numerical data by fitting a Lorentzian form in the neighborhood of $s=0$ ($t=0$) to the numerically generated data. Equations (46) and (49) relating the residues at $s=0$ or $t=0$ to the spectral densities summed over the nonzero s_i or t_i were found to hold to a fraction of a percent, i.e., running the simulation for a fixed value of p_1 generated F_0 and w_σ satisfying Eqs. (46) and (49) to a fraction of a percent. The limiting forms in Eqs. (44) and (45) for $s^2[F(s)-F_0(s)]\propto(1/V)\int d^3r|\theta_3(\vec{r})|$ and Eqs. (47) and (48) for $t^2[H(t)-H_0(t)]\propto(1/V)\int d^3r|\theta_3(\vec{r})|$ were also examined. For fixed δ/a the constants of proportionality are shown to agree to within a few percent provided that $a\ll L$. For $a\geqslant L$ the statistical correlations along the interface are affected by the finite width of the sample. In this limit the agreement of the constant of proportionality is less satisfactory.

In Fig. 1 the spectral density from $F(s)$ data is plotted as a function of $s=\sigma_2/(\sigma_2-\sigma_1)$. The effective conductivity data is obtained for systems with 50% σ_1 and 50% σ_2 for interfaces that average to the *y-z* plane. The results are labeled by δ and a characterizing the statistical properties in Eqs. (6) and (7) of the set of Gaussian random functions. In each figure two curves are presented representing results at fixed δ/a for two different sets of (δ,a). This gives an indication of the convergence of the numerically generated resistor network data to the continuum limit results. Units for δ and a are in resistor bond lengths, i.e., $\delta=1$ represents a δ of one bond length. In the plots presented, the ratio δ/a starts from a high value and decreases through one to a low value. This displays the behavior of the spectral density as one goes from the limit of surfaces that have high peaks falling quickly to narrow valley ($\delta/a\gg1$) to the limit of surfaces having smooth tapered hills ($\delta/a\ll1$). As expected, the spectral densities generated by the computer simulation are insensitive to the parallel shifting of the mean interface to the right or left of the *x-y* plane and to the corresponding percentage changes in σ_1 and σ_2 of the system. The rough interfaces generated by the simulation, however, must remain well contained within the finite volume of the resistor network treated by the simulation.

In general, for $\delta/a>1$ the spectral density is a broad flat function of s over the interval $0\leqslant s\leqslant1$. The flat region, which tends to narrow as $\delta/a=1$ is approached, is not featureless. It is composed of three rather low maxima with relatively large widths. For $\delta/a<1$ the spectral density continues to narrow reducing to a large peak centered at $s=\frac{1}{2}$ in the extreme $\delta/a\ll1$ limit. In the perturbation theory discussion given in Sec. IV, it will be shown that for $\delta/a\to0$ the density of states is a single pole at $s=\frac{1}{2}$. All of the results presented in Fig. 1 are symmetric about $s=\frac{1}{2}$. This comes from $F(s)-F_0(s)$ in Eq. (22) and the corresponding expression for $H(t)-H_0(t)$. Both $\sigma_0^{eff}-\sigma^{eff}$ and $\rho_0^{eff}-\rho^{eff}$ for large sized samples (i.e., $L\to\infty$) are determined by the properties of the systems in the vicinity of their random interfaces. Consequently, $\sigma_0^{eff}-\sigma^{eff}$ and $\rho_0^{eff}-\rho^{eff}$ should be invariant under the interchange of σ_1 and σ_2. For $F(s)-F_0(s)$ this implies that

$$\frac{1}{s}\sum_i \frac{F_i s_i}{s-s_i}=\frac{1}{s}\sum_i \frac{F_i s_i}{s-(1-s_i)}. \tag{51}$$

Similarly, from $H(t)-H_0(t)$ it follows that

$$\frac{1}{t}\sum_i \frac{H_i t_i}{t-t_i}=\frac{1}{t}\sum_i \frac{H_i t_i}{t-(1-t_i)}. \tag{52}$$

Both of these indicate symmetry under reflection through s or $t=\frac{1}{2}$.

The data from the finite network simulations leading to $F(s)$ are displayed in Table I. The sum rule $F_0-w_\sigma=p_1=0.5$ of Eq. (46) is evidently satisfied to a few parts per thousand. This provides a nontrivial evaluation of the accuracy of our simulations and of the errors introduced by the finiteness of the network ($L=128$) and its discrete nature. The values found for $C(\delta,a)\equiv\lim_{s\to\infty} s^2[F(s)-F_0(s)]$ of Eq. (44) satisfy the expectation that this quantity is proportional to $\delta^2/(La)$ for $\delta\ll a$ and to δ/L for $\delta\gg a$, which followed from Eq. (45) (see Sec. II C).

In Fig. 2, corresponding results for the spectral density from $H(t)$ of the effective resistivity with an interface which on average gives the *x-y* plane are presented. The spectral density is plotted as a function of $t=\rho_2(\rho_2-\rho_1)$ for the same range of δ and a values used to generate the data in Fig. 1. The same general features as found in the results (plotted versus s) in Fig. 1 are found for those (plotted versus t) in Fig. 2. (It should be noted that although the results in Figs. 1 and 2 exhibit general similarities if $t=s$, in fact $t\neq s$ are differently defined variables and the geometries of the two systems in Figs. 1 and 2 are quite different. Even if t were equal to s, the resulting figures are not the same, they are only similar in overall appearance and represent results for differently defined sets of spectral densities.) Once again the results should be symmetric about $t=\frac{1}{2}$ and, in the $\delta/a\ll1$ limit, the perturbation theory discussed in Sec. IV gives a spectral density with a single pole at $t=\frac{1}{2}$. It is interesting that the results in Figs. 1(e) and 2(e) are very similar in their respective dependences on s and t. This comes from the fact that in this limit the simple poles at $s=1/2$ or $t=1/2$ are dominating the respective behaviors of these systems in the weak perturbative limit.

The data from the finite network simulations leading to $H(t)$ are displayed in Table II. As was the case in Table I, the sum rule $H_0-w_\rho=p_1=0.5$ of Eq. (49) is usually satisfied to a

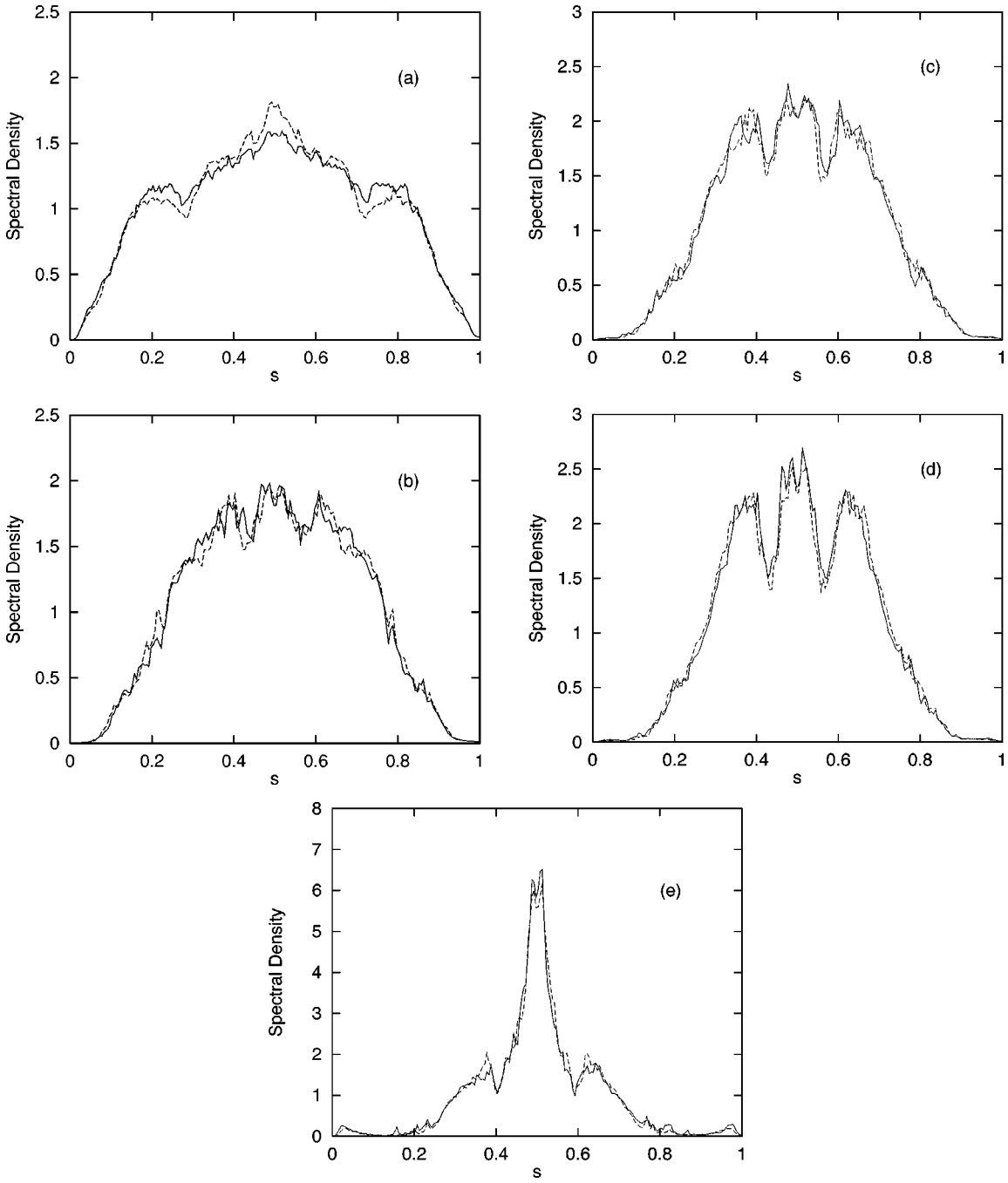

FIG. 1. A plot of the spectral density of $F(s)-F_0(s)$ divided by $C(\delta,a)$ versus s for (a) $\delta/a=4.00$ curves shown for $(\delta,a)=(8,2)$ (dashed line) and $(16,4)$ (solid line); (b) $\delta/a=1.33$ with curves shown for $(\delta,a)=(8,6)$ (dashed line) and $(12,9)$ (solid line); (c) $\delta/a=1.00$ with curves shown for $(\delta,a)=(12,12)$ (dashed line) and $(16,16)$ (solid line); (d) $\delta/a=0.75$ with curves shown for $(\delta,a)=(9,12)$ (dashed line) and $(12,16)$ (solid line); and (e) $\delta/a=0.25$ with curves shown for $(\delta,a)=(12,48)$ (dashed line) and $(16,64)$ (solid line).

few parts per thousand. Again, this provides a nontrivial evaluation of the accuracy of our simulations and of the errors introduced by the finiteness of the network ($L=128$) and its discrete nature. Again, as was the case in Table I, the values found for $R(\delta,a)\equiv\lim_{t\to\infty}t^2[H(t)-H_0(t)]$ of Eq. (47) satisfy the expectation that this quantity is proportional to $\delta^2/(La)$ for $\delta\ll a$ and to δ/L for $\delta\gg a$, which followed from Eq. (48) (see Sec. II C).

A consideration for both Figs. 1 and 2 is the effect of the size of the resistor array on the data. At the edges of the resistor array, the correlations along the random interface will be disrupted. This occurs on the interface within a correlation length of the edges of the array, even with the application of periodic boundary conditions. As a consequence, the effective correlation length of the generated data should be a little less than that for data that would be generated in an infinite system. These correlation length differences will be small (at most of order a/L) in the cases presented in Figs. 1 and 2. The spectral functions in Figs. 1 and 2, however, exhibit only small differences for changes in the correlation

TABLE I. Results for $F(s)$ from network simulations.

δ	a	$-w_\sigma$	F_0	F_0-w_σ	$C(\delta,a)$	$\frac{\delta}{2L}$	$\frac{\delta^2}{2La}$
8	2	0.093	0.406	0.499	0.0326	0.03125	0.125
16	4	0.180	0.318	0.498	0.0620	0.0625	0.25
8	6	0.064	0.436	0.500	0.0262	0.03125	0.04167
12	9	0.091	0.408	0.499	0.0376	0.046 875	0.0625
12	12	0.080	0.420	0.500	0.0339	0.046 875	0.046 875
16	16	0.104	0.395	0.499	0.0441	0.0625	0.0625
9	12	0.053	0.446	0.499	0.0233	0.035 156	0.026 367 2
12	16	0.069	0.431	0.500	0.0300	0.046 875	0.035 156 3
12	48	0.034	0.465	0.499	0.0143	0.046 875	0.011 718 8
16	64	0.044	0.453	0.497	0.0177	0.0625	0.015 625 0

length that are of the order of magnitude of those discussed above. On pages 10 and 11 of Ref. 38, a discussion of the formal treatment of finite size scaling effects arising in numerical simulations in terms of the dependence of the computed root mean square deviation of a property on the sample size is given. For the spectral densities of the systems treated in Figs. 1 and 2, such a discussion would be extremely computationally intensive and would not lead to new insight into the physics of these systems. It will not be pursued here.

Another type of interface that can readily be treated by the simulation technique and is of considerable interest is that of periodic interfaces. For this case the operators $\hat{\Gamma}_0$ and $\overleftrightarrow{\Gamma}_0$ in Eqs. (14) and (15) and Eqs. (33) and (34), respectively, exhibit the same periodicity as their buried interfaces. This follows from the complete translational symmetry of G_0, $\overleftrightarrow{G}_0$, ∇, $\nabla\times$, and the periodicity of the $\theta_1(\vec{r})$'s. Consequently, the eigenvalues and eigenvectors of Eqs. (14) and (33) obey Bloch's theorem: They form bands that are characterized by a Bloch **q**-vector that lies in the two-dimensional subspace (i.e., plane) of three-dimensional space, which embodies the periodic nature of the interface. These bands have gaps and other typical features, similar to those found in other physical systems that are characterized by spatial periodicity. However, only the $\mathbf{q}=0$ state from any Bloch band can contribute a nonzero weight F_i or H_i in the spectral expansion of $F(s)$ or $H(t)$. This statement, which is an exact theorem for continuum composites of infinite volume or periodic boundary conditions,[3,4] can be violated to some extent when we deal with finite sized discrete networks. For this reason, we included *all the eigenstates* whenever we calculated the spectral weight functions $g_\sigma(u)$, $g_\rho(v)$. Results of some of those calculations, using interfaces with periodic roughness, are reported below. A detailed treatment of the banding properties of the eigenstates for periodic interfaces will be presented in a future publication.

IV. PERTURBATION THEORY RESULTS

Perturbation theory can be used to obtain the effective conductivity (resistivity) of the buried interface problem as an expansion in the surface profile function. This is done separately for each of the cases treated in subsections II A and II B.

A. Average interface in the *y-z* plane

For this geometry, start from the current continuity equation $\nabla\cdot\vec{J}=0$ and write $\vec{J}=-\sigma(\vec{r})\nabla\phi$. The scalar function $\phi(\vec{r})$ then satisfies

$$\left[\frac{\partial^2}{\partial x^2}+\frac{\partial^2}{\partial z^2}\right]\phi(\vec{r})=0 \tag{53}$$

on either side of the interface. The boundary conditions for $L\to\infty$ on $\phi(\vec{r})$ are $\phi(z=-L/2)=0$, $\phi(z=L/2)=\phi_0$, and $\phi(\vec{r})$, and the normal component of $\vec{J}(\vec{r})$ are continuous at the random interface.

The solution for $\phi(\vec{r})$ can be written in the form

$$\phi^L(\vec{r})=\frac{1}{2}\phi_0\left(1+\frac{2z}{L}\right)+\sum_{n=0}^{\infty}D_1(n)\sin\left(\frac{2n\pi}{L}z\right)e^{(2n\pi/L)x}+\sum_{n=0}^{\infty}D_2(n)\cos\left[\frac{(2n+1)\pi}{L}z\right]e^{[(2n+1)\pi/L]x}, \tag{54}$$

for $x<\min\ \xi(z)$, and

$$\phi^R(\vec{r})=\frac{1}{2}\phi_0\left(1+\frac{2z}{L}\right)+\sum_{n=0}^{\infty}C_1(n)\sin\left(\frac{2n\pi}{L}z\right)e^{-(2n\pi/L)x}+\sum_{n=0}^{\infty}C_2(n)\cos\left[\frac{(2n+1)\pi}{L}z\right]e^{-[(2n+1)\pi/L]x}, \tag{55}$$

for $x>\max\ \xi(z)$. Here account is made of the boundary conditions at $z=\pm L/2$. In the application of the boundary conditions at the randomly rough interface, the Rayleigh hypothesis[33] is assumed to be valid. This assumption is that $x<\min\ \xi(z)$ in Eq. (54) can be replaced by $x<\xi(z)$, and that $x>\max\ \xi(z)$ in Eq. (55) can be replaced by $x>\xi(z)$. The Rayleigh hypothesis is generally found to be valid for Gaussian random systems in which $\delta/a<0.1$.

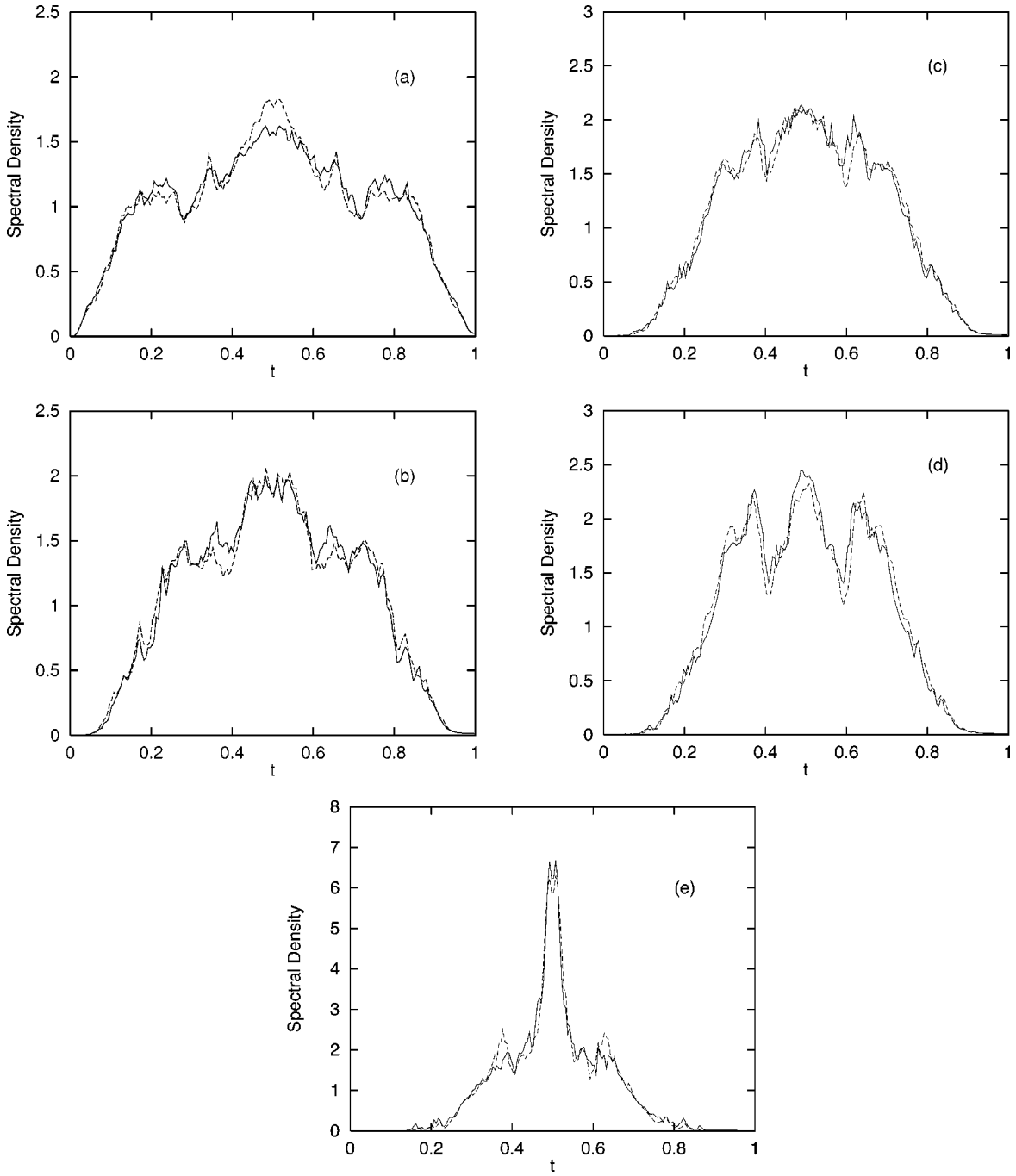

FIG. 2. A plot of the spectral density of $H(t)-H_0(t)$ divided by $R(\delta,a)$ versus t for (a) $\delta/a=4.00$ with curves shown for $(\delta,a)=(8,2)$ (dashed line) and $(16,4)$ (solid line); (b) $\delta/a=1.33$ with curves shown for $(\delta,a)=(8,6)$ (dashed line) and $(12,9)$ (solid line); (c) $\delta/a=1.00$ with curves shown for $(\delta,a)=(12,12)$ (dashed line) and $(16,16)$ (solid line); (d) $\delta/a=0.75$ with curves shown for $(\delta,a)=(9,12)$ (dashed line) and $(12,16)$ (solid line); and (e) $\delta/a=0.25$ with curves shown for $(\delta,a)=(12,48)$ (dashed line) and $(16,64)$ (solid line).

The first terms on the right-hand sides of Eqs. (54) and (55) are the solutions for ϕ^L and ϕ^R in the case of a flat interface. The remaining terms give the change from the flat interface results due to the random disorder in the interface. Consequently, the coefficients $D_1(n)$, $D_2(n)$, $C_1(n)$, and $C_2(n)$ depend on the surface roughness profile function $\xi(z)$ and vanish when $\xi(z)=0$. In the following, a perturbation expansion is generated by matching the interface boundary conditions in powers of the surface profile function $\xi(z)$.

To match the interface boundary conditions, the coefficients $C_\alpha(n)$ and $D_\alpha(n)$ for $\alpha=1$, 2 are written as series in powers of $\xi(z)$, so that

$$C_\alpha(n)=\sum_{i=1}^{\infty} C_{\alpha,i}(n) \tag{56}$$

and

TABLE II. Results from network simulations for $H(t)$.

δ	a	$-w_\rho$	H_0	H_0-w_ρ	$R(\delta,a)$	$\frac{\delta}{2L}$	$\frac{\delta^2}{2La}$
8	2	0.086	0.409	0.495	0.0310	0.03125	0.125
16	4	0.168	0.323	0.491	0.0606	0.0625	0.25
8	6	0.060	0.439	0.469	0.0246	0.03125	0.04167
12	9	0.087	0.412	0.499	0.0359	0.046 875	0.0625
12	12	0.075	0.424	0.499	0.0323	0.046 875	0.046 875
16	16	0.099	0.400	0.499	0.0424	0.0625	0.0625
9	12	0.050	0.450	0.500	0.0218	0.035 156	0.026 367 2
12	16	0.064	0.435	0.499	0.0284	0.046 875	0.035 156 3
12	48	0.028	0.470	0.498	0.0132	0.046 875	0.011 718 8
16	64	0.035	0.463	0.498	0.0165	0.0625	0.015 625 0

$$D_\alpha(n)=\sum_{i=1}^{\infty} D_{\alpha,i}(n). \tag{57}$$

Here $C_{\alpha,i}(n)$ and $D_{\alpha,i}(n)$ represent all contributions to these coefficients of order i in powers of ξ. Using Eqs. (56) and (57) in Eqs. (54) and (55), a system of equations for $D_{\alpha,i}$ and $C_{\alpha,i}$ are determined at the interface. These equations are used below to obtain the solutions for ϕ to first order in $\xi(z)$.

The continuity of $\phi(\vec{r})$ at $x=\xi(z)$ gives $\phi^L(\vec{r})|_{x=\xi(z)} = \phi^R(\vec{r})|_{x=\xi(z)}$. It then follows from Eqs. (54) and (55) that

$$C_{\alpha,1}(m)-D_{\alpha,1}(m)=0, \tag{58}$$

where $\alpha=1$ or 2. The continuity of the normal component of the current density at the random interface gives

$$\sigma_1\left(1,0,-\frac{d\xi}{dz}\right)\cdot\nabla\phi^L=\sigma_2\left(1,0,-\frac{d\xi}{dz}\right)\cdot\nabla\phi^R \tag{59}$$

for $x=\xi(z)$. From this and Eqs. (54) and (55) it follows that

$$\sigma_2 C_{1,1}(m)+\sigma_1 D_{1,1}(m)=\sigma_2-\sigma_1(\xi_{-m}+\xi_m)\frac{\phi_0}{L}, \tag{60}$$

and

$$\sigma_2 C_{2,1}(m)+\sigma_1 D_{2,1}(m)=\frac{\sigma_1-\sigma_2}{\sigma_1+\sigma_2}\frac{2}{(2n+1)\pi}\frac{\phi_0}{L}\int_{-L/2}^{L/2}dz \times\cos\left(\frac{(2n+1)\pi}{L}z\right)\frac{d\xi(z)}{dz}, \tag{61}$$

where $\xi(z)=\Sigma_p\xi_p e^{i(2p\pi z/L)}$.

Solving Eqs. (58), (60), and (61) gives $C_{1,1}(m)=D_{1,1}(m)$, $C_{2,1}(m)=D_{2,1}(m)$,

$$C_{1,1}(m)=\frac{\sigma_2-\sigma_1}{\sigma_1+\sigma_2}\frac{\phi_0}{L}(\xi_m+\xi_{-m}), \tag{62}$$

and

$$C_{2,1}(m)=\frac{\sigma_1-\sigma_2}{\sigma_1+\sigma_2}\frac{2}{(2n+1)\pi}\frac{\phi_0}{L}\int_{-L/2}^{L/2}dz \times\cos\left(\frac{(2n+1)\pi}{L}z\right)\frac{d\xi(z)}{dz}. \tag{63}$$

The z component of current density is then

$$J_z^{(1)}=-\sigma_1\frac{\phi_0}{L}-\sigma_1\frac{2\pi}{L}\sum_{n=0}^{\infty}\left[n\cos\frac{2n\pi}{L}zC_{1,1}(n)e^{(2n\pi/L)x} -\frac{2n+1}{2}\sin\frac{(2n+1)\pi}{L}zC_{2,1}(n)e^{[(2n+1)\pi/L]x}\right], \tag{64}$$

for $x<\xi(z)$, and

$$J_z^{(2)}=-\sigma_2\frac{\phi_0}{L}-\sigma_2\frac{2\pi}{L}\sum_{n=0}^{\infty}\left[n\cos\frac{2n\pi}{L}zC_{1,1}(n)e^{-(2n\pi/L)x} -\frac{(2n+1)}{2}\sin\frac{(2n+1)\pi}{L}zC_{2,1}(n)e^{-[(2n+1)\pi/L]x}\right], \tag{65}$$

for $x>\xi(z)$. The average current density for a given surface profile $\xi(z)$ is

$$J_{z,av}=\frac{1}{L}\int_{-L/2}^{L/2}\left[\frac{1}{L_1+\xi(z)}\int_{-L_1}^{\xi(z)}J_z^{(1)}dx +\frac{1}{L_2-\xi(z)}\int_{\xi(z)}^{L_2}J_z^{(2)}dx\right]dz, \tag{66}$$

where L_1 and $L_2\to\infty$ are the lengths of the σ_1 and σ_2 materials in the x directions. Averaging Eq. (66) over $\xi(z)$ gives the average current density $\langle\vec{J}\rangle$.

The average current density $\langle\vec{J}\rangle$ is computed from Eqs. (62)–(66) using

$$\langle\xi_m\xi_n\rangle=\frac{\sqrt{\pi}a\delta^2}{L}\exp-\left(\frac{\pi ma}{L}\right)^2\delta_{n+m,0}, \tag{67}$$

$$\langle(\xi_n+\xi_{-n})^2\rangle=\frac{\sqrt{\pi}a\delta^2}{L}\exp-\left(\frac{\pi na}{L}\right)^2(2+\delta_{-2n,0}+\delta_{2n,0}), \tag{68}$$

and

$$\sum_{n=0}^{\infty}f(2n+1)\approx\int_0^{\infty}dnf(2n+1). \tag{69}$$

Equation (69) has been used for functions $f(2n+1)$ which depend on $C_2(n)$. We find

$$\langle J_z\rangle=-\frac{L_1\sigma_1+L_2\sigma_2}{L_1+L_2}\frac{\phi_0}{L}+\frac{4}{L_1+L_2}\frac{(\sigma_2-\sigma_1)^2}{\sigma_1+\sigma_2}\frac{\phi_0}{L}\frac{\sqrt{\pi}\pi a\delta^2}{L^2}\sum_{n=0}^{\infty}n\exp-\left(\frac{\pi na}{L}\right)^2. \tag{70}$$

[Note: The general form of $\langle J_z\rangle$ in Eq. (70) for the case $L_1=L_2$ can be checked using a rough argument, originally given by Landau and Lifshitz for a bulk disordered medium. This is presented in the Appendix.] For equal concentrations of σ_1 and σ_2, in the $L\to\infty$ limit for $L_1=L_2=L/2$,

$$F(s)-F_0(s)=\frac{1}{\sqrt{\pi}}\frac{1}{s}\frac{1}{s-\frac{1}{2}}\frac{\delta}{L}\frac{\delta}{a}. \tag{71}$$

Here we use the definition of $F(s)$ and $F_0(s)$ in Eqs. (20)–(24).

The above expression has two simple poles at $s=0$ and $s=1/2$. We note that the singularities at these two values of s are generic features of the function $F(s)$ that appear for quite arbitrary microstructures: The pole at $s=0$ is a result of the fact that the subvolume of the σ_1 constituent percolates in the microstructure of Sec. II A, i.e., a continuous path through that constituent exists between the top and bottom equipotential plates.[6] The pole at $s=1/2$ is a result of the following mathematical property: Although the details of the pole spectrum of $F(s)$ (i.e., positions and residues) depend on the precise microstructure, that spectrum usually has an accumulation point at $s=1/2$, even if all the interfaces are smooth and regular and have no singular points.[5] Thus, in general, $F(s)$ will have an essential singularity at that point. The simple pole which we found at $s=1/2$, using perturbation theory, is the remnant of that essential singularity.

In the $L\to\infty$ limit for $L_1=L_2=L/2$, Eqs. (54)–(66) and (69) can be used to obtain $F(s)-F_0(s)$ for a general surface profile correlator $\langle\xi(z)\xi(0)\rangle$. We find that

$$F(s)-F_0(s)=-\frac{1}{2\pi}\frac{1}{s}\frac{1}{s-\frac{1}{2}}P\int dz\frac{1}{z}\frac{d}{dz}\langle\xi(z)\xi(0)\rangle. \tag{72}$$

Here the principal part $-(1/\pi)P\int dz(1/z)(d/dz)\langle\xi(z)\xi(0)\rangle=\int(dk/2\pi)|k|g(k)$, where in the $L\to\infty$ limit $\langle\xi(z)\xi(0)\rangle=\int(dk/2\pi)g(k)e^{ikz}$. Equations (54)–(66) and (69) can also be used to determine $F(s)-F_0(s)$ for interfaces that are nonrandom and periodic. For a periodic profile function of the form

$$\xi(z)=\sum_{n=0}^{\infty}\xi_n\cos\frac{2\pi n}{a}z+\sum_{n=1}^{\infty}\phi_n\sin\frac{2\pi n}{a}z, \tag{73}$$

$$F(s)-F_0(s)=\frac{\pi}{2}\frac{1}{s}\frac{1}{s-\frac{1}{2}}\left[2\frac{\xi_0^2}{La}+\sum_{n=1}^{\infty}\left(\frac{\xi_n^2}{La}+\frac{\phi_n^2}{La}\right)\right]. \tag{74}$$

B. Average interface in the *x-y* plane

For this geometry, the same formulation as that given in the first paragraph of Sec. IV A is used. The difference here, however, is that the average interface is in the *x-y* plane, not the *y-z* plane.

As the interface between the two components of the composite is not bounded in the *x-y* plane, the solution of Eq. (53) for $\phi(\vec{r})$ can now be written in the form

$$\phi^{>}(\vec{r})=A^{>}+B^{>}z+\int\frac{dk}{2\pi}e^{ikx}[C^{>}(k)e^{-kz}+D^{>}(k)e^{kz}], \tag{75}$$

where $z>\xi(x)$, and

$$\phi^{<}(\vec{r})=A^{<}+B^{<}z+\int\frac{dk}{2\pi}e^{ikx}[C^{<}(k)e^{-kz}+D^{<}(k)e^{kz}], \tag{76}$$

where $z<\xi(x)$. From the condition that $\phi(z=-L/2)=0$, it follows that

$$A^{<}=\frac{L}{2}B^{<} \tag{77}$$

and

$$D^{<}(k)=-C^{<}(k)e^{kL}. \tag{78}$$

Here again the Rayleigh hypothesis,[33] i.e., the representation of the solutions for $z>\xi(x)$ by the form valid for $z>\max\ \xi(x)$ and the solutions for $z<\xi(x)$ by the form valid for $z<\min\ \xi(x)$ is assumed. From the condition that $\phi(z=L/2)=\phi_0$, it follows that

$$\phi_0=A^{>}+\frac{L}{2}B^{>} \tag{79}$$

and

$$D^{>}(k)=-C^{>}(k)e^{-kL}. \tag{80}$$

Equations (77)–(80) are used to eliminate $B^{>}$, $B^{<}$, $D^{>}(k)$, and $D^{<}(k)$ from Eqs. (75) and (76), so that

$$\phi^{>}(\vec{r})=A^{>}+\frac{2}{L}(\phi_0-A^{>})z+\int\frac{dk}{2\pi}e^{ikx}C^{>}(k)[e^{-kz}-e^{-kL}e^{kz}] \tag{81}$$

and

$$\phi^{<}(\vec{r}) = A^{<}\left(1+\frac{2}{L}z\right) + \int \frac{dk}{2\pi} e^{ikx} C^{<}(k)[e^{-kz} - e^{kL}e^{kz}]. \tag{82}$$

The coefficients $A^{<}$, $A^{>}$, $C^{>}(k)$, and $C^{<}(k)$ are determined as functions of $\xi(x)$ by matching boundary conditions at the random interface.

The continuity of $\phi(\vec{r})$ and the component of $\vec{J}(\vec{r})$ normal to the interface at $z=\xi(x)$ gives

$$\phi^{>}[z=\xi(x)] = \phi^{<}[z=\xi(x)] \tag{83}$$

and

$$\sigma_2\left[-\frac{d\xi(x)}{dx},0,1\right]\cdot\nabla\phi^{>}(\vec{r}) = \sigma_1\left[-\frac{d\xi(x)}{dx},0,1\right]\cdot\nabla\phi^{<}(\vec{r}). \tag{84}$$

Expanding in powers of $\xi(x)$, we write

$$C^{i}(k) = \sum_{n=0}^{\infty} C_n^{i}(k), \tag{85}$$

where $i=>$ or $<$, and $C_n^{i}(k)$ represents terms of order n in ξ. Substituting Eqs. (81) and (82) into Eqs. (83) and (84) and using Eq. (85) gives

$$C_0^{>}(k) = 0, \tag{86}$$

$$C_1^{>}(k) = \frac{\sigma_1(\sigma_2-\sigma_1)}{(\sigma_2+\sigma_1)^2}\frac{1}{1-e^{-kL}}\frac{2\phi_0}{L}\hat{\xi}(k), \tag{87}$$

$$C_2^{>}(k) = \frac{\sigma_1(\sigma_2-\sigma_1)}{(\sigma_2+\sigma_1)^3}\frac{1}{e^{kL}-e^{-kL}}\frac{2\phi_0}{L}\left[(\sigma_1-\sigma_2)(e^{kL}+1)\times\int\frac{dq}{2\pi}q\frac{e^{qL}+1}{e^{qL}-1}\hat{\xi}(k-q)\hat{\xi}(q) + 2\sigma_2(e^{kL}-1)\times\int\frac{dq}{2\pi}q\hat{\xi}(k-q)\hat{\xi}(q)\right], \tag{88}$$

for the first three $C_n^{>}(k)$ coefficients. Here $\xi(x) = \int(dk/2\pi)e^{-ikx}\hat{\xi}(k)$. In the same way, the $C_n^{<}(k)$ coefficients are determined and found to be closely related to the $\{C_n^{>}(k)\}$. The $\{C_n^{<}(k)\}$ are obtained from the $\{C_n^{>}(k)\}$ by noting that $-C_n^{<}(k)$ is given from the expression for $C_n^{>}(k)$ by replacing L with $-L$ and interchanging σ_1 and σ_2. From Eqs. (83) and (84), the leading order terms in $\xi(x)$ give

$$A^{>} = A^{<} = \frac{\sigma_2}{\sigma_2+\sigma_1}\phi_0. \tag{89}$$

The effective conductivity is determined from the average current $\langle\vec{J}\rangle = -\langle\sigma(\vec{r})\nabla\phi(\vec{r})\rangle$. Using Eqs. (81), (82), and (85)–(88), the average z component of the current density is found to be

$$\langle J_z\rangle = -\frac{\sigma_2\sigma_1}{\sigma_2+\sigma_1}\frac{2\phi_0}{L}\left\{1+8\sqrt{\pi}\left[\frac{(\sigma_2-\sigma_1)}{(\sigma_2+\sigma_1)}\right]^2\left(\frac{\delta}{L}\right)^2\frac{a}{L}\times\int\frac{dr}{2\pi}r\frac{e^{2r}+1}{e^{2r}-1}\exp\left(-\frac{r^2a^2}{L^2}\right)\right\}. \tag{90}$$

In the $\delta=0$ limit this correctly reduces to the effective conductivity of the flat surface system. Using the relationship $\rho^{eff}=1/\sigma^{eff}$, the difference $H(t)-H_0(t)$, defined in Eqs. (40) and (43), to leading order in δ is

$$H(t)-H_0(t) = 2\sqrt{\pi}\frac{1}{t}\frac{1}{t-\frac{1}{2}}\left(\frac{\delta}{L}\right)^2\frac{a}{L}\int\frac{dr}{2\pi}r\frac{e^{2r}+1}{e^{2r}-1}\exp\left(-\frac{r^2a^2}{L^2}\right). \tag{91}$$

In the $L\to\infty$ limit

$$H(t)-H_0(t) = \frac{1}{\sqrt{\pi}}\frac{1}{t}\frac{1}{t-\frac{1}{2}}\frac{\delta}{L}\frac{\delta}{a}. \tag{92}$$

This has the same functional form as that of $F(s)-F_0(s)$ in Eq. (71).

Like Eq. (71), this expansion also has two simple poles at $t=0$ and $t=1/2$. These are generic features of the function $H(t)$: The pole at $t=0$ expresses the fact that the subvolume of the σ_2 constituent does not percolate between the top and bottom plates of the structure of Sec. II B.[6] In general, the point $t=1/2$ is an accumulation point of the pole spectrum of $H(t)$, and thus this function usually has an essential singularity at that point.[5] The simple pole that we obtained using perturbation theory is, again, the remnant of that essential singularity.

In addition, for a general surface profile correlator $\langle\xi(x)\xi(0)\rangle$,

$$H(t)-H_0(t) = -\frac{1}{2\pi}\frac{1}{t}\frac{1}{t-\frac{1}{2}}P\int dx\frac{1}{x}\frac{d}{dx}\langle\xi(x)\xi(0)\rangle,$$

which is the same form as Eq. (72) for $F(s)-F_0(s)$. For the nonrandom periodic surface given by

$$\xi(x) = \sum_{n=0}^{\infty}\xi_n\cos\frac{2\pi n}{a}x + \sum_{n=1}^{\infty}\phi_n\sin\frac{2\pi n}{a}x, \tag{93}$$

we get

$$H(t)-H_0(t) = \frac{\pi}{2}\frac{1}{t}\frac{1}{t-\frac{1}{2}}\left[2\frac{\xi_0^2}{La}+\sum_{n=1}^{\infty}\left(\frac{\xi_n^2}{La}+\frac{\phi_n^2}{La}\right)\right]. \tag{94}$$

C. Perturbation theory results

In the limit that $\delta\ll a\ll L$, the perturbation theory for $F(s)-F_0(s)$ and $H(t)-H_0(t)$ is very similar. The functional form of $F(s)-F_0(s)$ $[H(t)-H_0(t)]$ exhibits simple poles at $s=0(t=0)$ and $s=\frac{1}{2}(t=\frac{1}{2})$. These two poles are observed in the $\delta\ll a$ limit of the $s>0(t>0)$ data plotted in Fig. 1 (Fig. 2). Actually, at $s=1/2$ or $t=1/2$ there should be an essential singularity, as explained above.[5]

An interesting feature of the perturbation theory results is that both $F(s)-F_0(s)$ and $H(t)-H_0(t)$ are proportional to

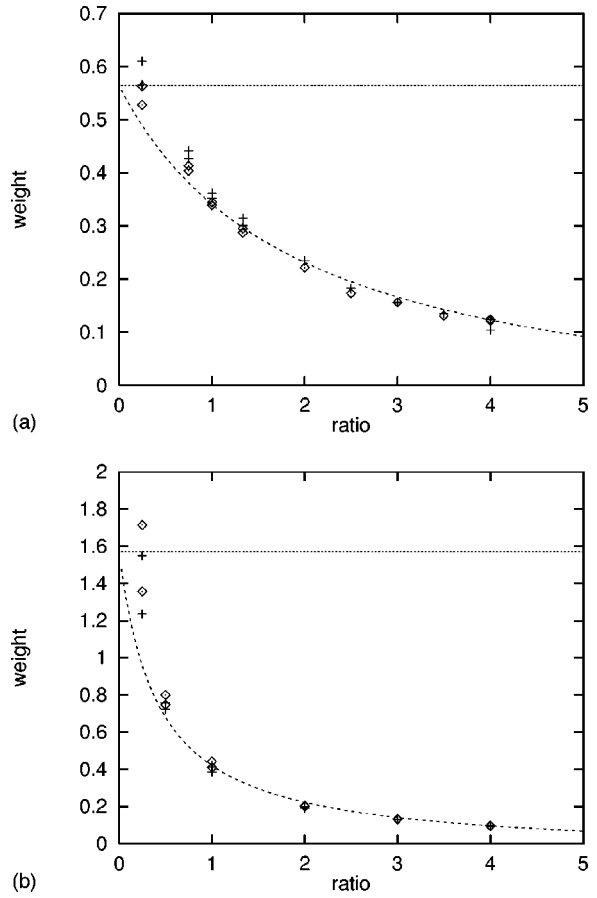

FIG. 3. Plot of the weight defined as $\lim_{s\to\infty} s^2[F(s)-F_0(s)]/(\delta^2/La)$ or $\lim_{t\to\infty} t^2[H(t)-H_0(t)]/(\delta^2/La)$ versus *ratio* $=\delta/a$ for (a) the Gaussian randomly rough interface and (b) the periodic cosine interface.

$\delta^2/(La)$. This suggests a scaling relation for $F(s)-F_0(s)$, $H(t)-H_0(t)$, and their sum rules. To see if this is the case, we have considered plots of the sum rules of $F(s)-F_0(s)$ and $H(t)-H_0(t)$ displaying such scaling.

In Fig. 3(a) plots of the sum rules in Eqs. (44) and (47) for Gaussian randomly rough interfaces are presented for various δ and a. The results are plotted so that the vertical scale shows $\lim_{s\to\infty} s^2[F(s)-F_0(s)]/(\delta^2/La)$ or $\lim_{t\to\infty} t^2[H(t)-H_0(t)]/(\delta^2/La)$ and the horizontal scale shows δ/a. The horizontal line indicates the perturbation theory limit and the dashed line is a Pade fit to the data. The Pade form used is $y=[1-0.8260(\delta/a)]/[\sqrt{\pi}+0.9179(\delta/a)]$, where y is on the vertical axis. This form forces the Pade form to a fit to the perturbation theory result $(1/\sqrt{\pi})$ in the $\delta/a=0$ limit. The numerically generated data lies on a universal curve given by the Pade form when plotted as described above. At small δ/a the numerically generated points closest to the Pade results are the ones with larger δ and a. This suggests that the discrepancy between the numerically generated data and the Pade form is mainly due to the discrete nature of the resistor network. [By this we mean that in modeling a continuum system by a discrete finite sized lattice, not all length scales are treated correctly (see a discussion of aliasing in Ref. 39). The numerical simulation of the lattice model does not accurately treat lengths less than the lattice constant and lengths greater than the lattice size. The continuum solutions, however, contain all length scales, although with varying degrees of importance. The limit $\delta/a\to 0$ is represented in the lattice by δ/a=(lattice constant)/(length of a side of the total lattice). This may differ form the $\delta/a\to 0$ limit of the continuum model.] The general decrease of the Pade form results in Fig. 3(a) with increasing δ/a is consistent with the discussions given below Eq. (45) for the dependence of p_3 on δ, a, and L. We remind the reader, however, that our computer data are limited by the discrete nature and finite size of the lattice.

In Fig. 3(b) a similar plot to that in Fig. 3(a) is given, but for periodic interfaces.[40] For these results the interfaces are given by $\xi(z)=\delta\cos(2\pi/a)z$ for the geometry of Sec. II A or by $\xi(x)=\delta\cos(2\pi/a)x$ for the geometry of Sec. II B. The data in Fig. 3(b) are scaled in the same manner as that in Fig. 3(a). The horizontal line gives the perturbation-limiting form, and the dashed line is a Pade fit with $y=[1.571-0.137(\delta/a)]/[1+2.414(\delta/a)]$ where y is the vertical axis, and y at $\delta/a=0$ is fixed on the value $\pi/2$ obtained from perturbation theory. The data fall on a universal curve given by the Pade form, and the discrepancies between the numerically generated data and the Pade form again seem to come from the effects of a discrete lattice. Again a decrease in the Pade form is observed with increasing δ/a, and this is consistent with out discussions of the dependence of p_3 on δ, a, and L.

An additional condition that σ^{eff} and ρ^{eff} must satisfy is the reciprocity relation.[10] This is a relation between σ^{eff} and ρ^{eff} defined on dual lattices. A good discussion of this relation can be found in Sec. 3.2 of Ref. 18. Since the square lattice is self-dual, the reciprocity relation relates the perturbation theory results for $F(s)$ and $H(t)$, so that $\sigma^{eff}(\sigma_1,\sigma_2,p_1)/\sigma_2=\sigma_1/\sigma^{eff}(\sigma_2,\sigma_1,p_1)=\rho^{eff}(\sigma_2,\sigma_1,p_1)/\rho_1$. This relation is satisfied by the perturbation results in Eqs. (71) and (92) since interchanging σ_1 and σ_2 in $t=\rho_2/(\rho_2-\rho_1)$ gives $t'=\rho_1/(\rho_1-\rho_2)=\sigma_2/(\sigma_2-\sigma_1)=s$. As the perturbation theory gives expressions for $F(s)$ and $H(t)$ that map into one another under interchanging s and t, the reciprocity relation is satisfied.

V. SURFACE PLASMONS AT A RANDOMLY ROUGH INTERFACE

In this section the long wavelength dispersion relation of surface plasmons on a one-dimensionally randomly rough dielectric interface is related to the functions $F(s)-F_0(s)$ and $H(t)-H_0(t)$. Two cases of surface plasmon propagation along the rough interface are treated: (a) propagation parallel to the grooves of the one-dimensional roughness and (b) propagation perpendicular to the grooves of the one-dimensional roughness. Applications of the relationship are given.

The propagation of surface plasmons along the random interfaces is considered for the geometries given in Secs. II A and II B. For the surface plasmon considerations, however, the material with conductivity σ_1 in Secs. II A and II B is replaced by a material with dielectric constant $\epsilon(\omega)$ and

the material with conductivity σ_2 is replaced by vacuum. Results for the resistor network can be used in the treatment of these two dielectric geometries, as in the continuum limit the conductivity problems studied in Secs. II and IV are isomorphic to the dielectric media problems. Replacing σ_1 by ϵ_1, σ_2 by ϵ_2, and σ^{eff} by ϵ^{eff} maps the two different problems onto one another so that results for one can be used to describe the other.

A. Dispersion relation: propagation parallel to the grooves

To relate $H(t)-H_0(t)$ to the surface plasmon dispersion relation for propagation parallel to the grooves of the one-dimensionally rough interface, consider the parallel plate geometry of Sec. II B. The region above the random interface is vacuum and the region below the interface is filled with an homogeneous isotropic dielectric characterized by $\epsilon(\omega)$. The potential difference between the plates in the following considerations is not fixed, but the system operates as a capacitor containing a quasistatic electric field. The surface plasmon modes treated in this geometry propagate in the y direction.

The upper plate has a quasistatic surface charge density, $q_s(x,y,\omega)$ of frequency ω, and the lower plate has a surface charge density $-q_s(x,y,\omega)$. The spatial variations of $q_s(x,y,\omega)$ are considered to be on length scales much larger than those characterizing the roughness of the randomly rough interface (i.e., δ, a). Consequently, the response of the system to $q_s(x,y,\omega)$ is determined by the effective dielectric properties of the random media, so that

$$\Delta V(x,y,\omega) = 4\pi L \frac{q_s(x,y,\omega)}{\epsilon^{eff}}, \tag{95}$$

where $\Delta V(x,y,\omega)$ is the potential between the plates at (x,y) and ϵ^{eff} is the effective dielectric constant. For a flat interface, Eq. (95) becomes

$$\Delta V_0(x,y,\omega) = 4\pi L \frac{q_s(x,y,\omega)}{\epsilon_0^{eff}}, \tag{96}$$

where the subscripts 0 indicate flat interface quantities. Here the charge densities $q_s(x,y,\omega)$ driving the systems in Eqs. (95) and (96) are the same. From Eqs. (95) and (96) it then follows that

$$\Delta V(x,y,\omega) - \Delta V_0(x,y,\omega) = 4\pi L\left(\frac{1}{\epsilon^{eff}} - \frac{1}{\epsilon_0^{eff}}\right) q_s(x,y,\omega). \tag{97}$$

The flat surface surface-plasmon of quasistatic frequency ω propagating in the y direction has an electric potential of the form

$$\phi(y,z,\omega) = (Ae^{-kz} + A_1 e^{k(z-L/2)})e^{iky} \tag{98}$$

above the interface, and

$$\phi(y,z,\omega) = (Be^{kz} + B_1 e^{-k(z+L/2)})e^{iky} \tag{99}$$

below the interface. Matching the boundary conditions at the interface and the surface charge density [i.e., $\pm q_s(y,\omega)$] boundary conditions at the upper and lower plates determines A, A_1, B, and B_1. (Notice that the charge density for a plasmon propagating in the y direction has no x dependence in the approximation used here.) From these coefficients it is found that

$$\Delta V_0(y,\omega) = 4\pi \frac{q_s(y,\omega)}{k}\left[\frac{1}{\epsilon(\omega)} + 1\right]\tanh(kL/2), \tag{100}$$

so that the difference in potential between the plates depends only on y.

Substituting Eq. (100) into Eq. (97) for large L gives

$$\Delta V(y,\omega) = 4\pi q_s(y,\omega)\frac{1}{k}\left\{\left[\frac{1}{\epsilon(\omega)} + 1\right] + kL\left(\frac{1}{\epsilon^{eff}} - \frac{1}{\epsilon_0^{eff}}\right)\right\}. \tag{101}$$

The condition for a surface plasmon mode to exist is that $\Delta V(y,\omega)=0$ for nonzero $q_s(y,\omega)$. This gives

$$\begin{aligned} 0 &= \frac{1}{\epsilon(\omega)} + 1 + kL\left(\frac{1}{\epsilon^{eff}} - \frac{1}{\epsilon_0^{eff}}\right) \\ &= \frac{1}{\epsilon(\omega)} + 1 - kL[H(t) - H_0(t)], \end{aligned} \tag{102}$$

where $t=\epsilon(\omega)/[\epsilon(\omega)-1]$ as the equation determining the surface plasmon dispersion relation on the random interface in the $L\to\infty$ limit. In the perturbation theory limit discussed in Sec. IV B, we find from Eqs. (92) and (102) that

$$0 = 1 - \frac{2}{\sqrt{\pi}}\frac{[\epsilon(\omega)-1]^2}{[\epsilon(\omega)+1]^2}\frac{\delta^2}{a}k \tag{103}$$

determines the surface plasmon dispersion relation at long wavelengths. The dispersion relation on the weakly random rough surface of Sec. IV B can also be computed from results of a Green's function scattering theory developed in Refs. 41 and 42. It is found that the dispersion relation from Refs. 41 and 42 is determined by

$$0 = 1 - \frac{2(1+\cos^2\theta)}{\sqrt{\pi}}\frac{[\epsilon(\omega)-1]^2}{[\epsilon(\omega)+1]^2}\frac{\delta^2}{a}k. \tag{104}$$

Here θ is the angle between the surface plasmon wave vector in the plane of the mean surface and the direction perpendicular to the grooves of the one-dimensionally randomly rough interface. Equations (103) and (104) are in agreement.

B. Dispersion relation: Propagation perpendicular to the grooves

To relate $F(s)-F_0(s)$ and $H(t)-H_0(t)$ to the surface plasmon dispersion relation for propagation perpendicular to the grooves of the one-dimensionally rough interface, consider the parallel plate geometry of Sec. II A. The plasmon now travels in the z direction. (Note that the discussions in this section are quite separate from those made in Sec. V A. Section V A treated the system described by the geometry in Sec. II B, whereas the discussion in this section is for a system described by the geometry in Sec. II A. These figures represent two distinct and different physical systems.) The

region to the left of the random interface is filled with an homogeneous isotropic dielectric characterized by $\epsilon(\omega)$ and the region to the right of the random interface is vacuum. The potential difference between the upper and lower plates is zero.

We consider the case in which the wavelength of the surface plasmon is much greater than the parameters a and δ characterizing the surface roughness. In this limit the response of the system to fields and charges far from the surface can be described in terms of an effective dielectric constant. The scalar potential of the surface plasmons with quasistatic frequency ω is then taken to be of the form

$$\phi(x,z,\omega) = f(kz)\phi_0(x,\omega), \tag{105}$$

where $f(kz)=\sin kz$ for $kL/2=n\pi$ or $f(kz)=\cos kz$ for $kL/2=(2n+1)\pi/2$ with $n=0,1,2,\ldots$ and

$$\phi_0(x,\omega) = Ae^{k(x+L/2)} \tag{106}$$

in the region to the left of the interface, with

$$\phi_0(x,\omega) = Be^{-k(x-L/2)} \tag{107}$$

in the region to the right of the interface.

From the discussion given in Sec. V A for plasmons moving in a system with the geometry of Sec. II B, it is expected from Eq. (95) that for $L' \gg \delta, a$,

$$\phi(x=L'/2,z,\omega) - \phi(x=-L'/2,z,\omega) = -\frac{L'D_x(x=L'/2,z,\omega)}{\epsilon^{eff}}. \tag{108}$$

Here $D_x(x=L/2,z,\omega)$ is viewed as being proportional to a surface charge density on a fictitious set of capacitor plates at $x=L'/2$ and $x=-L'/2$. The charge densities on the plates are equal in magnitude and opposite in sign. From Eqs. (105)–(108) it then follows that

$$A = B\left[1+\frac{kL'}{\epsilon^{eff}}\right]. \tag{109}$$

A second relationship between A and B can be obtained from $\int_{-\infty}^{\infty} dxD_z(x,z=-L/2,\omega)=0$. This is a statement that there is no net charge on the plate at $z=-L/2$ and follows from the boundary conditions $\phi(x,z=L/2,\omega)-\phi(x,z=-L/2,\omega)=0$. From Eqs. (105)–(107) we find that

$$0 = \int_{-\infty}^{\infty} dxD_z(x,-L/2,\omega) = -[\epsilon(\omega)A+B]\left.\frac{df}{dr}\right|_{r=-kL/2} - \int_{-L'/2}^{L'/2} dxD_z(x,-L/2,\omega), \tag{110}$$

and for $kL' \ll 1$ from $\langle D_z(x,-L/2,\omega)\rangle = \epsilon'^{eff}\langle E_z(x,-L/2,\omega)\rangle \approx -\epsilon'^{eff}kB(df/dr)|_{r=-kL/2}$ that

$$\int_{-L'/2}^{L'/2} dxD_z(x,-L/2,\omega) \approx -k\epsilon'^{eff}BL'\left.\frac{df}{dr}\right|_{r=-kL/2}. \tag{111}$$

In the above, ϵ'^{eff} is found by replacing ρ^{eff} by $1/\epsilon'^{eff}$, ρ_1 by $1/\epsilon(\omega)$, and ρ_2 by 1 in Eq. (40).

Equations (109)–(111) then give (setting $L'=L$)

$$\epsilon(\omega)+1 = -\epsilon(\omega)\frac{kL}{\epsilon'^{eff}} - kL\epsilon^{eff} \tag{112}$$

as the condition for a plasmon to exist on the rough interface. In terms of $H(t)-H_0(t)$ for $t=\epsilon(\omega)/[\epsilon(\omega)-1]$ and $F(s)-F_0(s)$ for $s=1/[1-\epsilon(\omega)]$ Eq. (112) becomes

$$0 = [\epsilon(\omega)+1] - kL\{\epsilon(\omega)[H(t)-H_0(t)] + F(s)-F_0(s)\} \tag{113}$$

for $kL \ll 1$. In the perturbation theory limit discussed in Sec. IV, Eq. (113) yields

$$0 = 1 - \frac{4}{\sqrt{\pi}}\frac{[\epsilon(\omega)-1]^2}{[\epsilon(\omega)+1]^2}\frac{\delta^2}{a}k \tag{114}$$

as the condition determining the surface plasmon dispersion relation. This agrees with the results in Eq. (104), which was obtained by another method.[41,42]

C. Effective boundary conditions for one-dimensionally rough interfaces

It is interesting to note that the above results for surface plasmon propagation on a one-dimensionally randomly rough interface, in the limit of long wavelength, can be obtained by representing the effects of the interface roughness by a set of effective boundary conditions defined over the plane of the mean random interface.

Consider a random dielectric-vacuum interface described by the surface profile function $z=\xi(x)$. Let us replace the rough interface and its boundary conditions by a smooth surface at $z=0$ supporting a position-dependent effective surface polarizations.[43] This polarization is chosen so as to reproduce the results in Eqs. (102) and (113). To do this, the effective surface polarization is taken to be a vector field with x and z components defined by

$$P_{s,x}(x) = \chi_x E_x[x,\xi(x)^+], \tag{115}$$

where $P_{s,x}(x)$ is the x component of polarization per area located at $(x,z=0)$, $\chi_x(x)$ is the susceptibility at $(x,z=0)$, $E_x[x,\xi(x)^+]$ is the x component of the electric field in the vacuum above the surface, and by

$$P_{s,z}(x) = \chi_z E_z[x,\xi(x)^+] \tag{116}$$

for the corresponding z components of the quantities occurring in Eq. (115). There is no roughness in the y direction, so that the y component of effective surface polarization is zero, i.e., $\chi_y(x)=0$. The susceptibilities for determining the average fields above and below the interface are then written in terms of $F(s)-F_0(s)$ and $H(t)-H_0(t)$ as

$$4\pi\chi_x = -L[F(s)-F_0(s)] \tag{117}$$

and

$$4\pi\chi_z = L[H(t)-H_0(t)]. \tag{118}$$

Here $t=\epsilon(\omega)/(\epsilon(\omega)-1)$, $s=1/[1-\epsilon(\omega)]$, $\epsilon(\omega)$ is the dielectric constant of the medium below the random interface, and

$L \to \infty$ is the separation of the two parallel plates used in the determination of $F(s)-F_0(s)$ and $H(t)-H_0(t)$.

The boundary conditions at the $z=\xi(x)$ interface are replaced by effective boundary conditions on the $z=0$ plane which are written in terms of the effective surface polarizations defined in Eqs. (115)–(118). The new boundary conditions at $z=0$ are from $\nabla \times \vec{E}=0$ given by

$$0 = E_x^+(x) - E_x^-(x) + 4\pi \frac{\partial P_{s,z}(x)}{\partial x}, \tag{119}$$

where $E_x^+(x)$ and $E_x^-(x)$ are the average electric fields immediately above and below the $z=0$ interface, and from $\nabla \cdot \vec{D}=0$ given by

$$0 = D_z^+(x) - D_z^-(x) + 4\pi \frac{\partial P_{s,x}(x)}{\partial x}, \tag{120}$$

where $D_z^+(x)$ and $D_z^-(x)$ are the average displacement fields immediately above and below the $z=0$ interface respectively. Using these conditions to compute the dispersion relations of the surface plasmons reproduces the results in Sec. V A and V B.

D. Electron energy loss for motion parallel to a surface

Recently Mendoza *et al.*[44] (see also Refs. 45–47) have developed a theory for determining the small energy losses of electrons with energies of order of 100 KeV moving parallel to a dielectric surface. The mean dielectric surface is taken at the $z=0$ plane with the dielectric in the region above the plane and vacuum below the plane, and the electron moves with position coordinates $(x=0, y=vt, z=-z_0)$. (Note: This is slightly different from the other treatments given in this paper which have taken the dielectric to be below the surface. To facilitate the discussions here, we shall use the geometry and notation in Mendoza *et al.*[44] in this subsection.) The losses arise from the polarization of the dielectric medium, and are related to the surface response function, $g(Q,-z_0,\omega)$, defined by

$$\phi^{ind}(\vec{Q},-z_0,\omega) = -g(Q,-z_0,\omega)\phi^{ext}(\vec{Q},z_0,\omega). \tag{121}$$

Here $\phi^{ext}(\vec{Q},-z_0,\omega)$ is the spectral component of the electric potential from the electron in the case that no dielectric medium is present, and in position-frequency space we have

$$\phi^{ext}(\vec{\rho},z;\omega) = \int \frac{d^2Q}{(2\pi)^2}\phi^{ext}(\vec{Q},\omega)e^{i\vec{Q}\vec{\rho}+Qz}, \tag{122}$$

where $\vec{\rho}=(x,y)$ is a two-dimensional vector parallel to the interface. The potential $\phi^{ind}(\vec{Q},-z_0,\omega)$, which in position-frequency space is given by

$$\phi^{ind}(\vec{\rho},z;\omega) = \int \frac{d^2Q}{(2\pi)^2}\phi^{ind}(\vec{Q},\omega)e^{i\vec{Q}\vec{\rho}-Qz}, \tag{123}$$

is the induced electric potential in the $z=-z_0$ plane due to the interaction of the electron with the dielectric medium above the interface. In the following, the surface response function for a rough interface, $g(Q,-z_0,\omega)$, will be expressed in terms of $F(s)-F_0(s)$ and $H(t)-H_0(t)$ for electron motions parallel and perpendicular to the grooves of the one-dimensionally rough interface. Given these expressions, Eqs. (6) and (7) of Ref. 44 can be used to compute the probability per unit path length, per unit energy, of the electron scattering with energy loss $E=h\omega$.

To compute $\phi^{ind}(\vec{\rho},z;\omega)$ the effective boundary conditions of Sec. V C are used. The electric quasistatic potential in the presence of the surface roughness is given throughout space by

$$\phi_r(\vec{\rho},z;t) = \int \frac{d^2Q}{(2\pi)^2}e^{i\vec{Q}\cdot\vec{\rho}}\phi(z)e^{-i\omega t}\Big|_{\omega=Q_y v}, \tag{124}$$

where

$$\phi(z) = Ae^{-Qz} \tag{125}$$

for $z>0$, and

$$\phi(z) = B_1 e^{-Q(z+z_0)} + B_2 e^{Q(z+z_0)} \tag{126}$$

for $0>z>-z_0$ (here the B_2 term is the induced potential seen by the electron), and

$$\phi(z) = Ce^{Q(z+z_0)} \tag{127}$$

for $z<-z_0$. The boundary conditions for the determination of A, B_1, B_2, and C are (a) at $z=-z_0$, $\partial\phi^+/\partial z-\partial\phi^-/\partial z=4\pi e$, $\phi^+=\phi^-$, (b) at $z=0$ Eqs. (119) and (120), and (c) at $z \to \pm\infty$ the fields are zero.

Solving the boundary value problem gives

$$\phi^{ext}(\vec{Q},-z_0;\omega) = \frac{-2\pi e}{Q} \tag{128}$$

and

$$\phi^{ind}(\vec{Q},-z_0;\omega) = B_2, \tag{129}$$

where

$$B_2 = \frac{2\pi e}{Q}\frac{\epsilon(\omega)-1+4\pi Q[\epsilon(\omega)\chi_z + Q_x^2\chi_x/Q^2]}{\epsilon(\omega)+1+4\pi Q[-\epsilon(\omega)\chi_z + Q_x^2\chi_x/Q^2]}e^{-2Qz_0}, \tag{130}$$

and

$$g(\vec{Q},\omega) = -\frac{B_2}{B_1}. \tag{131}$$

In the limit $\omega/v \to 0$ for motion parallel to the grooves,

$$e^{2Qz_0}g(\vec{Q},\omega) = \frac{\epsilon(\omega)-1+LQ\{\epsilon(\omega)[H(t)-H_0(t)]-F(s)+F_0(s)\}}{\epsilon(\omega)+1-LQ\{\epsilon(\omega)[H(t)-H_0(t)]+F(s)-F_0(s)\}}, \tag{132}$$

where $t=\epsilon(\omega)/[\epsilon(\omega)-1]$ and $s=1/[1-\epsilon(\omega)]$. In the same limit for motion perpendicular to the grooves, a solution similar to that outlined above gives

$$e^{2Qz_0}g(\vec{Q},\omega)=\frac{\epsilon(\omega)-1+LQ\epsilon(\omega)[H(t)-H_0(t)]}{\epsilon(\omega)+1-LQ\epsilon(\omega)[H(t)-H_0(t)]}. \tag{133}$$

E. Reflection of *p*-polarized electromagnetic waves from a one-dimensionally randomly rough surface near normal incidence

It has been important to us in our discussions of $F(s)-F_0(s)$ and $H(t)-H_0(t)$ to show that these functions are not just mathematical curiosities, but that they are related to a number of physically measurable and important properties of surfaces. In this section, the functions $F(s)-F_0(s)$ and $H(t)-H_0(t)$ are also related to the reflectivity of *p*-polarized light near normal incidence from one-dimensionally randomly rough interfaces. This is a very basic optical property of rough surfaces.

In these considerations, we treat electromagnetic waves of quasistatic frequency ω incident from vacuum onto a dielectric medium that is uniform, isotropic, and characterized by a dielectric constant $\epsilon(\omega)$. The plane of incidence is taken to be either parallel or perpendicular to the grooves of the one-dimensionally random interface. We assume that the wavelength $\lambda \gg \delta, a$ and only calculate the specular reflection, but not diffuse scattering.

1. Plane of incidence perpendicular to the grooves of the one-dimensional surface

In the considerations given here the *x*-*y* plane is the mean plane of the vacuum-dielectric interface.

On a flat vacuum-dielectric interface, the Fresnel coefficient for the reflection of *p*-polarized light is[41,42]

$$R_0(p)=\frac{\epsilon(\omega)\alpha_0(p\omega)-\alpha(p\omega)}{\epsilon(\omega)\alpha_0(p\omega)+\alpha(p\omega)}. \tag{134}$$

Here p is the component of the wave vector of the incident planewave of electromagnetic radiation in the *x*-*y* plane, $\alpha_0(p\omega)=[\omega^2/c^2-p^2]^{1/2}$, and $\alpha(p\omega)=[\epsilon\omega^2/c^2-p^2]^{1/2}$ with Re $\alpha(p\omega)$, Im $\alpha(p\omega)>0$. For the rough interface scattering geometry of this section, Eqs. (8), (13b), and (17) of Ref. 42 give an average Fresnel coefficient of the form

$$R_r(p)=\frac{\epsilon(\omega)\alpha_0(p\omega)-\alpha(p\omega)+i\epsilon(\omega)M(p)}{\epsilon(\omega)\alpha_0(p\omega)+\alpha(p\omega)-i\epsilon(\omega)M(p)}. \tag{135}$$

Here the average Fresnel coefficient of the rough interface is defined from Eq. (8) of Ref. 42 by $\langle R(p|k)\rangle=2\pi\delta(p-k)R_r(p)$ and $M(p)$ (Given in the pole approximation in Eq. (17) of Ref. 42.) is the self-energy correction of the average single particle Green's function for surface plasmon propagation on the rough interface. (The Green's function is averaged over the random roughness of the interface.) The average Greens function for the propagation of a surface plasmon of wavevector p and frequency ω on the random interface, $G(p\omega)$, is given in terms of $M(p)$ by

$$G(p\omega)=1/\{[G_0(p\omega)]^{-1}-M(p)\}. \tag{136}$$

Here $G_0(p\omega)=i\epsilon(\omega)/[\epsilon(\omega)\alpha_0(p\omega)+\alpha(p\omega)]$ is the surface plasmon Green's function for propagation on a flat surface.

Using $M(k)$ from Eqs. (18) and (19) of Ref. 42 and Eq. (135) evaluated at normal incidence gives

$$R_r(p=0)=\frac{\epsilon(\omega)-\epsilon(\omega)^{1/2}+i\epsilon(\omega)(\omega/c)M_0}{\epsilon(\omega)+\epsilon(\omega)^{1/2}-i\epsilon(\omega)(\omega/c)M_0}, \tag{137}$$

where

$$M_0=-\frac{2}{\sqrt{\pi}}\frac{1}{\epsilon(\omega)^2}\frac{[\epsilon(\omega)-1]^2}{\epsilon(\omega)+1}\frac{\sigma^2}{a}=-L\frac{F(s)-F_0(s)}{\epsilon(\omega)^2}. \tag{138}$$

The correction M_0 due to surface roughness scattering is seen to be divergent at $\epsilon(\omega)=0$ and $\epsilon=-1$. These singularities are prominent in determining the effects of surface roughness on the reflectance at normal incidence. The results in Eqs. (137) and (138) agree in the limit that $\epsilon\to-1$ with the reflectivity results to leading order in the surface roughness calculated using the boundary conditions in Sec. V C.

2. Plane of incidence parallel to the grooves of the one-dimensional surface

To obtain the Fresnel coefficient for light incident in an arbitrary plane of incidence perpendicular to the one-dimensionally rough interface, Eq. (135) and results in Ref. 41 can be used. Reference 41 contains expressions for the Green's function describing the propagation of surface plasmons along the interface at an arbitrary angle to the grooves of the one-dimensionally rough interface. These expressions give the self-energy M_0 in the limit of weak roughness. The resulting Fresnel coefficient is obtained from Eq. (137) with M_0 of the form

$$M_0=-\frac{2}{\sqrt{\pi}}\frac{1}{\epsilon(\omega)^2}\frac{[\epsilon(\omega)-1]^2}{\epsilon(\omega)+1}\sin^2\phi_i\frac{\sigma^2}{a}$$
$$=-L\frac{F(t)-F_0(t)}{\epsilon(\omega)^2}\sin^2\phi_i. \tag{139}$$

Here ϕ_i is the angle between the magnetic field of the incident electromagnetic wave and the direction perpendicular to the grooves of the grating. At $\phi_i=\pi/2$ the results in Eqs. (138) and (139) are found to agree, to leading order in the interface roughness, with the reflectivity computed using the boundary conditions of Sec. V C.

3. Evaluation of reflectivity for ion crystals

In this subsection Eqs. (137)–(139) are evaluated for a vacuum-CdS interface at normal incidence of light. Results are presented for magnetic field polarizations parallel and perpendicular to the grooves of a one-dimensionally random rough surface. In these evaluations the dielectric function of CdS is given by the form[48]

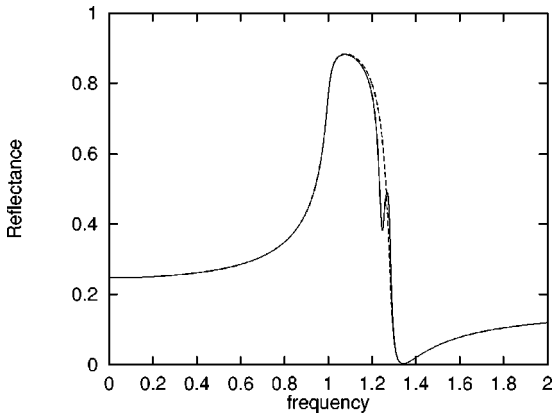

FIG. 4. Plot of the reflectance versus frequency (ω/ω_t) for CdS. Results are shown for the case in which the magnetic field of the incident light is parallel (solid) and perpendicular (dashed) to the grooves of the one-dimensionally rough interface.

$$\epsilon(\omega) = \epsilon_0 \frac{\omega_l^2 - \omega^2 - i\omega_c\omega}{\omega_t^2 - \omega^2 - i\omega_c\omega}, \tag{140}$$

where $\epsilon_0 = 5.4$, $\omega_t = 232.0\ \mathrm{cm}^{-1}$, $\omega_l = 298.0\ \mathrm{cm}^{-1}$, and $\omega_c = 6.9\ \mathrm{cm}^{-1}$.[48]

Results are presented in Fig. 4 for the reflectivity versus frequency. The one-dimensionally rough surface is Gaussian random characterized by $\omega_t\sigma = 0.1$ and $\omega_t a = 1.0$. For the case in which the magnetic field is parallel to the grooves of the one-dimensionally rough surface a dip in the reflectance at $\omega/\omega_t = 1.243$ is observed. This arises from the singularity in Eq. (138) at $\epsilon(\omega) = -1$. Aside from this feature the reflectance is little changed from the unperturbed reflectance. For the case in which the magnetic field is perpendicular to the grooves of the one-dimensionally rough surface $\phi_i = 0$ in Eqs. (139) and the reflectance is given by the unperturbed reflectance.

VI. LAYERED INTERFACES

In certain instances the results presented above for single interfaces should generalize to systems of multiple interfaces that on average are parallel to one another. For interfaces that are at separations far from each other, it is expected that each interface can be separately viewed as interacting with an effective medium which accounts for the average effects of the other interfaces on the system. This should be the case when the average separation between the interfaces is much greater than the parameters characterizing the surface roughness. In this limit a given interface in the system sees only an average effect of the electric field fluctuations created by the presence of its neighboring random interfaces. To facilitate this picture of multiple random interfaces we will develop below an effective circuit representation for single interfaces and then suggest a generalization to multiple interfaces.

It is interesting to note from Eq. (24) that if both σ_1 and σ_2 are real and positive, then $s < 0$ or $s > 1$ and $F(s) - F_0(s) > 0$. From Eq. (22) this indicates that the conductance of the system with an average interface in the y-z plane is decreased by interface roughness. The effective interface conductance, σ_{int}^{eff}, defined by $\sigma_{int}^{eff} = \sigma^{eff} - \sigma_0^{eff}$, is seen to be negative, and for weakly rough surfaces $|\sigma_{int}^{eff}|$ is small. A useful way of viewing the system in terms of an equivalent electrical circuit is to think of the layer of conductance σ_1, the layer of conductance σ_2, and the interface with interface conductance σ_{int}^{eff} as a set of three parallel resistors across which a constant potential is applied. For small $|\sigma_{int}^{eff}|$ (i.e., large interface resistances) the resistance of the system is dominated by the layers of σ_1 and σ_2. Only when $|\sigma_{int}^{eff}|$ becomes large does it significantly affect the properties of the system. A drawback of this equivalent circuit representation is that the effective interface resistance is negative. It is expected that the equivalent circuit representation is easily generalizable to a system of multiple interfaces that are on mean parallel to the y-z plane and that in this case the multiple interfaces at sufficient interface separations add like parallel resistors.

An explanation of the decrease in the effective conductivity of the system with a rough interface from the smooth surface case comes from an examination of the region along the x axis that bounds the random interface [see Fig. 5(a)]. For the smooth interface, this region consists of a layer of high conductivity and a layer of low conductivity. The current flow is set by the layer of high conductivity. For the random interface all linear paths between the plates at $z = L/2$ and $z = -L/2$ intersect materials of both high and low conductivity. This reduces the net conductivity in this region.

For $H(t) - H_0(t)$ we note from Eq. (43) that if both ρ_1 and ρ_2 are real and positive, then $H(t) - H_0(t) > 0$ for $t < 0$ and $t > 0$. The resistance of two slabs connected in series is, consequently, always decreased by interface roughness, and from Eqs. (40) and (41) the effective interface resistivity $\rho_{int}^{eff} = \rho^{eff} - \rho_0^{eff}$ is found to be negative. An equivalent circuit representation for this slab geometry is that of three resistors in series. These represent the layer of resistivity ρ_1, the layer of resistivity ρ_2, and the resistivity of the interface layer. A drawback in this equivalent circuit representation is that the effective resistivity of the interface layer is negative, but the equivalent series resistor representation should be directly generalizable to a system of multiple interfaces that are on mean parallel to the x-y plane and at sufficient interface separations form one another.

In these systems the effective resistivity is decreased from the smooth surface results due to surface roughness. This arises due to the tongues of low resistivity media that protrude into the regions which would otherwise, in the smooth surface system, contain high resistivity material [see Fig. 5(b)]. These tongues provide low resistivity paths that lower the effective resistivity of the system with a random interface.

The limiting factor on the equivalent circuit representation is the effects of surface roughness fluctuations at one surface on the potential seen at another surface. An estimate of the importance of fluctuations in the interface roughness on the interaction between interfaces can be made by considering the potential at the mean surface of an interface due to a small localized fluctuation on a neighboring interface. We consider how a cylindrical fluctuation that maintains the average surface field and profile on one interface affects the

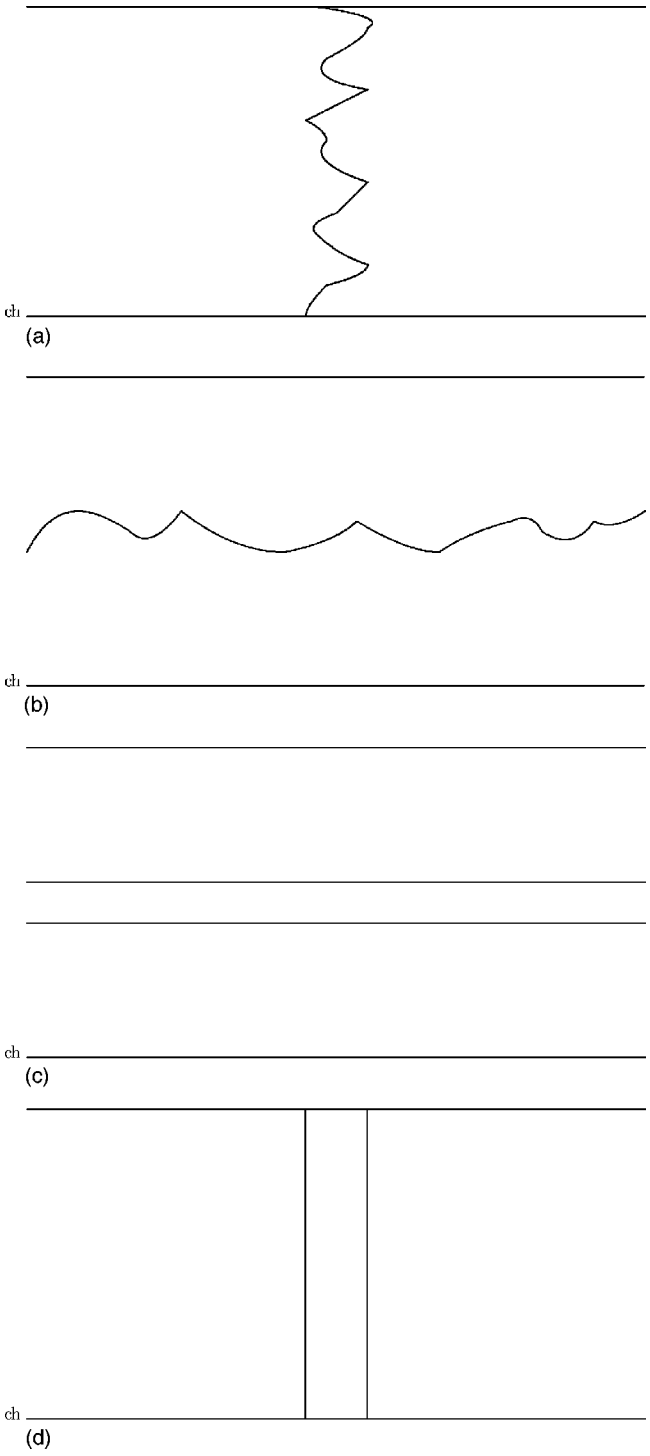

FIG. 5. Schematic plots for a single random interface: (a) vertical and (b) horizontal. The horizontal is the x direction and the vertical is the z direction. Schematic plot for two interfaces. The horizontal is the x direction and the vertical is the z direction. (c) Two horizontal interfaces separated by d_2. (d) Two vertical interfaces separated by d_2. In both figures the applied potential is across the horizontal upper most and lower most plates.

potential on a neighboring interface. It is well known that the potential from a dielectric cylinder of radius a in a uniform applied electric field $E\hat{k}$ is $V_{dipole} \propto (S/r)E \cos\theta$, where $S = \pi a^2$ is the cross-sectional area of the cylinder and (r,θ) are polar coordinates with θ measured relative to $\hat{k}$. This potential form generalizes in the limit of far fields for a cylinder of arbitrary bounded cross sectional shape of area S. Next consider two adjacent interfaces in a layered medium. The potential difference between the two inner interfaces in the geometry of Fig. 5(c) is $\Delta\phi \propto d_2 E$, where E is the average field at the mean interface. A fluctuation on the lower interface can be modeled as a set of two cylinder dipoles of cross-sectional areas δa (here δ and a define the Gaussian random surface profile statistics) that are oppositely directed along the $\hat{k}$ direction. One dipole cylinder is located at $(x = -a/2, z = \delta/2)$ relative to a coordinate system whose origin lies on the mean surface of the lower interface and the other is located at $(x = a/2, z = -\delta/2)$. The intensity of the dipole moment on each of the two cylinders is taken to be proportional to $\delta a E$. The electrostatic potential on the upper interface at a point adjacent to the a surface fluctuation on the lower interface is then approximately $\Delta\phi_{dipole} \propto \delta^2 a E/d_2^2$. The ratio $\Delta\phi_{dipole}/\Delta\phi \propto \delta^2 a/d_2^3$ must be small for the interfaces to be treated in an equivalent resistor scheme that ignores the detailed effects of surface fluctuations on adjacent interfaces. A similar argument can be applied to the geometry in Fig. 5(d). Here two dipoles oppositely directed along the $\hat{k}$ direction are located at $(x = \delta/2, z = a/2)$ and $(x = -\delta/2, z = -a/2)$ relative to a coordinate system whose origin lies on the mean surface of the left hand interface. On the right-hand interface, separated by a distance d_2 form the left-hand interface, the potential adjacent to this fluctuation is $\Delta\phi_{dipole} \propto \delta a^2 E/d_2^2$. The change in electrostatic potential observed in moving a distance comparable to d_2 in the $\hat{k}$ direction is $\Delta\phi \propto d_2 E$. For the effects of the fluctuations to be small, again $\Delta\phi_{dipole}/\Delta\phi = \delta a^2/d_3^2$ must be small.

Another way of arriving at an estimate of the effects of surface fluctuations on the interaction between adjacent interfaces is to treat the surface roughness on an interface as a position dependent dipole distribution on the mean plane of the interface. The total dipole moment averages to zero over the interface. For the case in Fig. 5(c), let the lower of the two embedded interfaces have a dipole density given by $p(x)$ with Gaussian random statistics, i.e., $\langle p(x)\rangle = 0$ and $\langle p(x)p(x')\rangle = (\delta p)^2 \exp[-(x-x')^2/a^2]$, where $\langle\ \rangle$ indicates an average over the surface. If the separation between the two interfaces is d_2 and the mean plane of the lower interface is at $z = 0$, then in the $d_2 \gg a$ limit it follows that $\langle E^2(x, z = d_2)\rangle / \langle E^2(x, z = 0)\rangle \propto [a/d_2]^3$. This agrees with the power law dependence obtained in the previous paragraph.

VII. CONCLUSION

A study has been presented of the spectral densities of two-component composites with buried random interfaces for both effective conductivity and resistivity systems. Analytical limiting forms and perturbation theory results have been used in conjunction with numerical results from resistor network studies to determine the dependence of the spectral densities on the statistical properties of the buried interface.

It is found in both effective conductivity (resistivity) systems that for $\delta/a \geqslant 1$ the spectral density is a broad plateau

function of s (t) in the region $0<s<1(0<t<1)$. Three low broad maxima are observed over the plateau and as δ/a approaches 1 the plateau narrows. For $\delta/a \ll 1$ the spectral densities in both effective conductivity and resistivity systems for $0<s<1(0<t<1)$ approach a single isolated pole at $s=\frac{1}{2}(t=\frac{1}{2})$. Data generated from numerical simulation are found to exhibit the analytical limiting forms predicted by the Bergman-Milton theory.

The spectral densities numerically generated for periodic interfaces are found to exhibit features distinct from those of the densities generated for randomly rough interfaces. Evidence of a band structure is seen in the numerical data which, for finite sized systems, appears to be given by a clustering of simple poles.

Both the effective conductivity and resistivity systems can be modeled in terms of effective circuits of resistors. In the effective conductivity system the equivalent circuit is that of parallel resistors, while the effective resistivity system has an equivalent circuit of series resistors. This simple modeling is expected to generalize to systems of buried interfaces which are parallel upon interface averaging, and the simulation results for the effective surface resistivity and conductivities are expected to be of use in studying more complicated buried interface geometries than those used for their computation.

The functions $F(s)-F_0(s)$ and $H(t)-H_0(t)$ are shown to be related to a number of problems in surface physics. These include the determination of the renormalization of the surface plasmon dispersion due to interface roughness, the energy losses of moving charged particles due to surface polarization, and the reflectivity of electromagnetic waves at rough interfaces in the weak roughness limit. Recent experiments on the electron-energy loss[49] and the reflectivity[50] of silver particles deposited on a substrate have identified features related to surface plasmon-polaritons. These results seem to be consistent with the gross features expected from the theory presented in Sec. V (i.e., anomalies in these functions associated with plasmon-polaritons), but are for systems that are two-dimensionally random and composed from three different dielectric components. Our theories are for one-dimensionally random surfaces composed from two different dielectric components. Nonetheless, we hope that future experimental efforts can be directed to one-dimensionally rough surfaces of a type that will allow for a quantitative comparison with the results presented in this paper.

ACKNOWLEDGMENTS

This work was supported by NSF grant DMR0078361. A.R.M. would like to thank the Department of Physics and Astronomy, Michigan State University, and the Center for Fundamental Materials Research, Michigan State University, for support during the work on this project. Partial support for the research of D.J.B. was provided by grants from the US-Israel Binational Science Foundation and the Israel Science Foundation. D.J.B. would also like to acknowledge the hospitality and support of the Department of Physics and Astronomy, Michigan State University, where this project was initiated.

APPENDIX: GENERAL FORM OF EQ. (70)

A rough check on the form in Eq. (70) for the current can be made using a treatment based on a discussion given by Landau and Lifshitz[51] of the effective permittivity of bulk dielectric mixtures. The arguments in Ref. 51 for a bulk media are closely followed in the discussion given below of interfaces.

Consider the geometry in Sec. II A used for the derivation of $F(s)$ in Sec. IV A. Define the current in the system by $\vec{J}(x,z)=\vec{J}_0+\delta\vec{J}(x,z)$, where $\vec{J}_0=\int d^3r\vec{J}(x,z)/V$ is the volume average of $\vec{J}(x,z)$ and $\delta\vec{J}(x,z)$ is the fluctuation from the volume average current. Likewise, the electric field is $\vec{E}(x,z)=\vec{E}_0+\delta\vec{E}(x,z)$ and the conductivity is $\sigma(x,z)=\sigma_0+\delta\sigma(x,z)$. Ohm's law then reads $\vec{J}(x,z)=[\sigma_0+\delta\sigma(x,z)][\vec{E}_0+\delta\vec{E}(x,z)]$, so that upon averaging,

$$\vec{J}_0=\sigma_0\vec{E}_0+[\delta\sigma\delta\vec{E}]_0, \tag{A1}$$

where $[\cdots]_0$ indicates a volume average. An approximation for $[\delta\sigma\delta\vec{E}]_0$ is now obtained.

From $\nabla\cdot\vec{J}=0$ it follows that

$$\sigma_0\nabla\cdot\delta\vec{E}+\vec{E}_0\cdot\nabla\delta\sigma=0, \tag{A2}$$

where only terms of first order in the small parameter are retained. Noting that $\delta\vec{E}=(\delta E_1,0,\delta E_3)$ and assuming a local average of a specific realization of a random surface, Eq. (A2) gives

$$\delta E_3=-\frac{E_{30}}{\sigma_0(1+\alpha)}\delta\sigma, \tag{A3}$$

where $E_{30}=[E_3]_0$ and α is a constant arising from the anisotropy of the interface geometry. It follows that

$$[\delta\sigma\delta E_3]_0=-\frac{E_{30}}{\sigma_0(1+\alpha)}[(\delta\sigma)^2]_0, \tag{A4}$$

so that the effective conductivity is given by

$$\sigma^{eff}=\sigma_0-\frac{[(\delta\sigma)^2]_0}{\sigma_0(1+\alpha)}. \tag{A5}$$

The spatial averaged value of the conductivity appearing in Eq. (A5) is given by $\sigma_0=(\sigma_1+\sigma_2)/2$. An estimate of $[(\delta\sigma)^2]_0$ in Eq. (A5) can be obtained in the $\delta/a<1$ limit using the fact that the effective conductivity of the system must be invariant under the interchange of the regions of conductivity σ_1 and σ_2. Likewise, the effective conductivity must be invariant under a sign change of the amplitude δ of the surface disorder. This, however, is not the case with the correlation length of the statistical fluctuations of the random surface, which must always be positive. The effective conductivity should then display terms linear in a. Taking these considerations together, along with the fact that the effective conduc-

tivity equals σ_0 when $\delta=0$ or $a=0$ or $\sigma_1=\sigma_2$, we find that $[(\delta\sigma)^2]_0=\beta(a\delta^2/L^3)(\sigma_1-\sigma_2)^2$, where L is the length of the interface and β is a constant. From Eq. (A5) then

$$\sigma^{eff}=\frac{\sigma_1+\sigma_2}{2}-2\beta\frac{a\delta^2}{L^3}\frac{(\sigma_1-\sigma_2)^2}{(1+\alpha)(\sigma_1+\sigma_2)}. \qquad \text{(A6)}$$

This agrees with the form of σ^{eff} obtained from Eq. (70) in the $\delta/a\ll 1$, $L_1=L_2$ limit.

It is interesting to note that in the case of a two-dimensionally randomly rough surface, $\delta\vec{E}=(\delta E_1,\delta E_2,\delta E_3)$, which leads to a change in the denominator on the left-hand side of Eq. (A6), replacing $1+\alpha$ by $1+2\alpha$. If, as with the homogeneous on average media $\alpha=1$, this would give a factor of $1/2$ in Eq. (A6) for the one-dimensionally rough surface and a factor of $1/3$ in Eq. (A6) for the two-dimensionally rough surface. The arguments above should give a rough indication of the behavior of the conductivity of the system in the perturbation limit.

[1] A. Sihvola, *Electromagnetic Mixing Formulas and Applications* (The Institute of Electrical Engineers, London, 1999).
[2] D. J. Bergman, Phys. Rep., Phys. Lett. **43**, 377 (1978).
[3] D. J. Bergman, Phys. Rev. B **19**, 2359 (1979).
[4] D. J. Bergman, J. Phys. C **12**, 4947 (1979).
[5] D. J. Bergman, *Bulk physical properties of composite media*, in Les méthodes de l'homogénéisation: Théorie et applications en physiques (Editions Eyrolles, Paris, 1985); Lecture Notes from the EDF Summer School on Homogenization Theory in Physics and Applied Mathematics, Bréau-sans-Nappe, France, June–July 1983, pp. 1–128.
[6] D. J. Bergman and D. Stroud, *Solid State Physics*, edited by H. Ehrenreich and D. Turnbull (Academic, New York, 1992), Vol. 46, pp. 147–269.
[7] D. J. Bergman, Ann. Phys. (San Diego) **138**, 78 (1982).
[8] G. W. Milton, Appl. Phys. Lett. **37**, 300 (1980).
[9] G. W. Milton, J. Appl. Phys. **52**, 5286 (1981).
[10] G. W. Milton, J. Appl. Phys. **52**, 5294 (1981).
[11] R. Fuchs, Phys. Rev. B **11**, 1732 (1975).
[12] R. Fuchs and S. H. Lui, Phys. Rev. B **14**, 5521 (1976).
[13] S. Kirkpatrick, Rev. Mod. Phys. **45**, 574 (1973).
[14] D. J. Frank and C. J. Lobb, Phys. Rev. B **37**, 302 (1988).
[15] R. Tao, Z. Chen, and P. Sheng, Phys. Rev. B **41**, 2417 (1990).
[16] L. C. Shen, C. Liu, J. Korringa, and K. J. Dunn, J. Appl. Phys. **67**, 7071 (1990).
[17] D. J. Bergman and K. J. Dunn, Phys. Rev. B **45**, 13 262 (1992).
[18] A. R. Day and M. F. Thorpe, J. Phys.: Condens. Matter **8**, 4389 (1996).
[19] A. R. Day and M. F. Thorpe, J. Phys.: Condens. Matter **11**, 2551 (1999).
[20] K. Ghosh and R. Fuchs, Phys. Rev. B **38**, 5222 (1988).
[21] R. Fuchs and F. Claro, Phys. Rev. B **39**, 3875 (1989).
[22] K. Hinsen and B. U. Felderhof, J. Chem. Phys. **94**, 5655 (1991).
[23] K. Hinsen and B. U. Felderhof, Phys. Rev. B **46**, 12 955 (1992).
[24] A. R. Day and M. F. Thorpe, J. Phys.: Condens. Matter **8**, 4389 (1996).
[25] K. P. Yuen, M. F. Law, and K. W. Yu, Phys. Rev. E **56**, R1322 (1997).
[26] T. Jonckheere and J. M. Luck, J. Phys. A **31**, 3687 (1998).
[27] Y. V. Fydorov, J. Phys. A **32**, 7429 (1999).
[28] H. Ma and P. Sheng, Phys. Rev. B **61**, 962 (2000).
[29] C. Noguey and R. G. Barrera, Phys. Rev. B **57**, 302 (1998).
[30] C. E. Roman-Velazquez, C. Noguez, and R. G. Barrera, Phys. Rev. B **61**, 10 427 (2000).
[31] A. R. Day, M. F. Thorpe, A. R. Grant, and A. J. Sievers, Physica A **19**, 17 (2000).
[32] A. R. Day, A. R. Grant, A. J. Sievers, and M. F. Thorpe, Phys. Rev. Lett. **84**, 1978 (2000).
[33] A. R. McGurn, Surf. Sci. Rep. **10**, 357 (1990).
[34] S. Simeonov, A. R. McGurn, and A. A. Maradudin, Proc. SPIE **3141**, 152 (1997).
[35] K. Golden and G. Papanicolaou, Commun. Math. Phys. **90**, 473 (1983).
[36] K. Golden, J. Mech. Phys. Solids **34**, 333 (1986).
[37] D. J. Bergman, SIAM (Soc. Ind. Appl. Math.) J. Appl. Math. **53**, 915 (1993).
[38] D. W. Heermann, *Computer Simulation Methods in Theoretical Physics*, 2nd ed. (Springer, Berlin, 1990), pp. 10 and 11.
[39] J. Honerkamp, *Statistical Physics: An Advanced Approach with Applications* (Springer, Berlin, 1998), Chap. 9.
[40] B. Laks, D. L. Mills, and A. A. Maradudin, Phys. Rev. B **23**, 4965 (1981).
[41] A. R. McGurn and A. A. Maradudin, J. Opt. Soc. Am. B **10**, 539 (1993).
[42] A. R. McGurn, A. A. Maradudin, and V. Celli, Phys. Rev. B **31**, 4866 (1985).
[43] J. D. Jackson, *Classical Electrodynamics*, 3rd ed. (Wiley, New York, 1999).
[44] C. I. Mendoza, R. G. Barrera, and R. Fuchs, Phys. Rev. B **57**, 11 193 (1998).
[45] R. G. Barrera and R. Fuch, Phys. Rev. B **52**, 3256 (1995).
[46] R. Fuch, R. G. Barrera, and J. L. Carrillo, Phys. Rev. B **54**, 12 824 (1996).
[47] K. L. Kliewer and R. Fuch, Phys. Rev. **172**, 607 (1968).
[48] M. P. Marder, *Condensed Matter Physics* (Wiley, New York, 2000), pp. 616–619.
[49] R. Lazzari, J. Jupille, and J.-M. Layer, Phys. Rev. B **68**, 045428 (2003).
[50] R. Lassari, S. Roux, I. Simonsen, J. Jupille, D Bedeaux, and J. Vlieger, Phys. Rev. B **65**, 235424 (2002).
[51] L. D. Landau and E. M. Lifshitz, *Electrodynamics of Continuous Media* (Pergamon, Oxford, 1960), p. 45.